Trend Inflation and the Phillips Curve in Emerging Economies

Dony Alex*

December 10, 2025

Abstract

This paper investigates the evolving inflation-output dynamics in a set of large emerging economies using a time-varying Phillips curve framework with stochastic trends and cycles. Our findings indicate a structural divergence in the drivers of inflation: trend inflation remains the dominant driver in Brazil, whereas the inflation gap has become the primary driver in India, South Africa, and post-2010 Mexico, signaling successful anchoring. We also find that the adoption of inflation targeting has generally contributed to lower levels of trend inflation; however, recent data reveals a rising contribution of trend shocks in Chile and Indonesia, pointing to emerging risks to anchoring. While evidence from advanced economies points to a persistently flatter Phillips curve, our results reveal considerable fluctuations in the slope across emerging economies, with curves remaining steep and volatile in Brazil and South Africa. Furthermore, a decomposition of the cyclical component reveals that Brazil is unique in having inflation dynamics driven primarily by the output gap (demand), whereas supply-side residual factors dominate in the other economies. Output gaps in all economies turned sharply negative during major global crises, with COVID-19 producing deeper and more persistent downturns than the global financial crisis, and with recovery paths proving highly asymmetric across countries.

1 Introduction

"If you put it in a murder mystery framework – "Who Killed The Phillips curve?"– it was the Fed that killed the Phillips curve." : James Bullard [President of the Federal Reserve Bank of St. Louis]: NPR, October 29, 2018.

The Phillips curve remains a cornerstone in the analytical frameworks used by central banks to understand inflation dynamics. At its core, the Phillips curve links economic slack, often measured by the output gap to inflation through wage and cost pressures. In principle, stronger demand raises wages, which in turn pushes up prices. However,

*O. P Jindal Global University. Email Address: dalex@jgu.edu.in

recent empirical evidence has cast doubt on the strength of this relationship. A number of studies find that univariate time-series models forecast inflation more accurately than multivariate Phillips curve specifications (Stock and Watson, 2007; Dotsey, Fujita, and Stark, 2018). This weak relationship between inflation and economic slack has been interpreted as evidence of a "flattening" of the Phillips curve, prompting some to argue that the relationship has become dormant, or even obsolete (Ball and Mazumdar, 2011; Coibion and Gorodnichenko, 2015; Blanchard, Cerutti, and Summers, 2015). The apparent flattening of the Phillips curve carries important policy implications, as it suggests that demand management policies may have limited influence on inflation outcomes. One explanation advanced for this phenomenon is the increased anchoring of long-term inflation expectations under stable monetary regimes. If current inflation dynamics are largely determined by long-term expectations, then the role of output gaps or other measures of slack diminishes substantially (Bernanke, 2007; Mishkin, 2007; Hazell et al., 2020). This underscores the importance of incorporating expectations and persistent components of inflation into empirical models.

Inflation dynamics in emerging economies exhibit notable differences from those observed in advanced economies. Whereas inflation in advanced economies tends to follow relatively stable and predictable patterns, emerging economies are often characterized by heightened volatility, recurrent structural breaks, and significant data limitations. Consequently, empirical modeling of inflation in emerging economies necessitates a framework that incorporates three critical features: (i) a potentially non-linear relationship between inflation and economic slack, (ii) the capacity to capture regime shifts and structural changes in the economy, and (iii) a robust measure of trend inflation that reflects the central bank's long-run inflation objective. Moreover, cost-push shocks frequently play a dominant role in EMEs, making it crucial to distinguish between transitory fluctuations and persistent inflationary pressures when assessing underlying dynamics.

While the New Keynesian Phillips Curve (NKPC) offers a microfounded rationale for these dynamics, its empirical estimation has been fraught with challenges (Fuhrer, 1997; Gali and Gertler, 1999; Roberts, 2001). As noted in the literature, ordinary least squares (OLS) estimations are subject to simultaneity bias, as output gaps are often negatively correlated with cost-push shocks (McLeay and Tenreyro, 2020; Barnichon and Mesters, 2021). Furthermore, estimations using the generalized method of moments (GMM) have been criticized because the forward-looking inflation expectations term introduces weak identification, often attributing spurious dominance to forward-looking behavior even when backward-looking dynamics prevail (Mavroeidis, 2005). Thus, the coexistence of three sources of endogeneity—unobserved inflation expectations, unobserved output gaps, and confounding supply shocks, renders conventional approaches unreliable. To overcome these challenges, this paper develops a flexible unobserved components model that explicitly captures stochastic trends and cyclical gaps, mitigating these identification prob-

lems and offering a robust characterization of inflation dynamics in emerging economies.

Motivated by this insight, we develop an empirical framework based on a state-space representation of the NKPC with time-varying parameters. Specifically, we incorporate both time-varying trend inflation and time-varying trend output into a reduced-form NKPC framework. This paper provides new estimates for the time-varying trend inflation and time-varying trend output for emerging economies in a model approximating a NKPC. This specification is advantageous in two respects. First, it accommodates latent state variables such as trend inflation and output, which cannot be directly observed but are critical for understanding underlying inflationary pressures. Second, the state-space approach is well-suited to emerging markets where data limitations, gaps, and measurement issues are common.

A primary motivation for this approach is the need to distinguish between genuine structural inertia and shifts in the long-run trend. Conventional specifications that measure inflation relative to a fixed steady state often exaggerate persistence, creating a "persistence puzzle" that necessitates the ad-hoc inclusion of backward-looking terms. To address this, we model inflation in "gap form"—defined as the deviation of actual inflation from a time-varying trend. Following Cogley and Sbordone (2008), this specification attributes most observed persistence to shifts in the central bank's long-run inflation target rather than intrinsic price-setting inertia.

The importance of modeling trend inflation lies in its close association with monetary regimes and central banks' long-term inflation targets (Cogley and Sbordone, 2008). Empirical studies show that shifts in trend inflation often signal changes in monetary policy frameworks (Cecchetti et al., 2007; Morley, Piger, and Rasche, 2015). Our approach also links inflation dynamics to central bank credibility and the anchoring of inflation expectations. Since all countries in our sample have adopted inflation-targeting regimes, we can compare the evolution of credibility across regimes. Following Cogley, Primiceri, and Sargent (2010), we interpret the persistence of the inflation gap as a measure of credibility with values close to zero indicating strong credibility, while values approaching one suggest weaker credibility. To ensure that this parameter remains economically meaningful, we constrain it within the interval $0 < \rho_t < 1$. Building on Chan, Koop, and Potter (2016), we model inflation gap persistence as a bounded random walk, reflecting the institutional constraints imposed by inflation-targeting central banks. Our framework embeds credibility and anchoring directly within the inflation process, offering a richer characterization of inflation dynamics in emerging economies.

The paper contributes to the literature on inflation dynamics in emerging economies through the prism of stochastic trend and cycles. While recent literature has extensively examined inflation anchoring in emerging markets—using survey data decay functions for Latin America (Gondo and Yetman, 2018), financial market break-even rates for Brazil, Chile, and Mexico (De Pooter et al., 2014), or unobserved component models focused on

Asian economies, this paper advances this body of work by integrating these regional perspectives into a unified, time-varying Phillips curve framework. Unlike Garcia and Poon (2022), who utilize survey expectations to identify trend inflation , this study relies on a structural Phillips curve linked to the output gap. This methodological distinction reveals both alignments and divergences; for instance, while both studies confirm strong credibility and a dominance of transitory shocks for India , they diverge on Indonesia, where Garcia and Poon (2022) find stability , whereas this framework detects a rising contribution of trend inflation shocks in the latter sample. Behera et al. (2018) validate the existence of a conventional Phillips curve in India by utilizing a panel of sub-national data and finding that excess demand conditions and exchange rate depreciation significantly harden consumer price inflation. Beyond trend estimation, this study contributes novel evidence on the heterogeneity of the Phillips curve slope—finding that while curves have flattened in Chile and Mexico, they remain steep and volatile in Brazil and South Africa and extends the analysis to capture the asymmetric recovery paths following the COVID-19 pandemic.

The paper also contributes to the literature on Phillips curve estimation with output gap derived from unobserved components models (Kuttner, 1994; Basistha and Startz, 2008; Planas, Rossi and Fiorentini, 2008; Jarociński and Lenza, 2018).While prior studies have focused primarily on advanced economies, the evidence for emerging markets remains limited. We fill this gap by providing new estimates of time-varying trend inflation and trend output for a set of emerging economies, and by documenting the role of both trend inflation and the inflation gap (defined as the deviation of actual inflation from its trend) in shaping inflation dynamics. Furthermore, we examine time variation in the slope of the Phillips curve and changes in inflation-gap persistence, thereby offering new insights into the evolving inflation–output tradeoff in emerging economies.

Our results reveal important cross-country differences in inflation dynamics among emerging economies. We find that inflation targeting regimes have generally lowered trend inflation and reduced the volatility of trend shocks. Mexico and South Africa exhibit improved anchoring of long-term expectations, while Brazil remains an outlier with weakly anchored expectations. Output gaps turn sharply negative during global crises, with post-COVID recovery uneven across countries. The slope of the Phillips curve exhibits substantial time variation being relatively flat in Chile, Mexico, and post-2015 India, but steep and volatile in Brazil and South Africa, hence highlighting heterogeneous inflation–output tradeoffs. Interpreting inflation-gap persistence as a credibility measure, India and (post-2005) South Africa exhibit low persistence consistent with stronger credibility, while Brazil, Chile, and Indonesia show high or unstable persistence, indicating weaker policy credibility. Crucially, variance decompositions reveal a divergence in the drivers of inflation: while the inflation gap has become the dominant driver in India, South Africa, and post-2010 Mexico (signaling strong anchoring), trend inflation accounts

for a growing share of variation in Chile and Indonesia, joining Brazil where permanent trend shocks remain the primary driver of inflation dynamics.

The remainder of the paper is structured as follows. Section 2 outlines the empirical model employed in the analysis. Section 3 describes the data and discusses the estimation strategy. Section 4 presents the main results and provides a detailed analysis of different components of the model. Section 5 reports the variance decomposition, highlighting the relative contributions of trend inflation and the inflation gap to overall inflation dynamics. Finally, Section 6 concludes with the key findings and policy implications.

2 Model

This section presents the empirical model, which is a bivariate unobserved component model. First, we decompose inflation into a random walk trend component π^*, capturing the impact of permanent shocks on inflation, and inflation gap π^g as stationary stochastic cycle which is given as,

$$\pi_t = \pi_t^* + \pi_t^g \tag{1}$$

Trend inflation follows a driftless random walk,

$$\pi_t^* = \pi_{t-1}^* + \epsilon_t^{\pi^*} \tag{2}$$

To capture changes in the volatility of shocks to trend inflation, we allow stochastic volatility in the innovation to the inflation trend.

$$\epsilon_t^{\pi^*} \sim N(0, e^{g_t})$$

Trend component can be interpreted as the limiting forecast of inflation as the forecast horizon goes to infinity following Beveridge and Nelson(1981)[1].

$$\pi_t^* = \lim_{s \to \infty} \mathbb{E}_t[\pi_{t+s} | I_t] \tag{3}$$

where s is the expectation horizon and I_t is the information set at time t.

Thus, π_t^* approximates the central bank's long-run inflation target, while deviations π_t^g capture short- run cyclical pressures.

We also decompose the quarterly GDP as a trend and cycle representation, where output gap is modelled as the deviation of output from trend output.

(4)

$$y_t = y_t^* + x_t$$

Identification is challenging for the hybrid Phillips curve. For identification of the Phillips curve we will require more lags in output gap than the lags in the measurement equation (Harvey, 2014). So we allow outptut gap to follow an $AR(2)$ process following the unobserved component literature on modelling output gap (Lee and Nelson, 2007; Jarocinski and Lenza, 2018).

$$x_t = \phi_1 x_{t-1} + \phi_2 x_{t-2} + \epsilon_t^x \tag{5}$$

where Φ_1 and Φ_2 are constant parameters and ϵ_t^x is $i.i.d.N(0, \sigma_x^2)$.

Trend ouput also follows a random walk process assuming persistence in the output for these emerging economies. Unlike most of the literature on emerging economies which use ad-hoc detrending or use fixed filters such as Hodrick-Prescott filter, we use a model consistent way to estimate trend output. A substantial literature with UC models has modelled the trend output as a random walk with drift. But an issue with this representation is that it assumes trend output growing at a constant rate. Breaks in trend output have been found for these emerging economies, so we use a trend specification which has a time-varying growth rate. For this trend output we use a second order integrated(local-linear) trend,

$$\Delta y_t^* = \Delta y_{t-1}^* + \epsilon_t^{y^*} \tag{6}$$

where $\epsilon_t^{y^*}$ is $i.i.d.N(0, \sigma_{y^*}^2)$

Following Cogley and Sbordone (2008), we model the NKPC in gap form, measuring inflation relative to its time-varying trend. This specification attributes most observed persistence to shifts in the central bank's long-run inflation target rather than intrinsic price-setting inertia, allowing a purely forward-looking NKPC to fit the data without ad hoc backward-looking terms and yielding a more policy-relevant link between inflation, marginal costs, and expectations..

$$\pi_t^g = \rho_t \pi_{t-1}^g + \lambda_t x_t + \epsilon_t^\pi \tag{7}$$

where $\pi_t^g = \pi_t - \pi_t^*$ and $x_t = y_t - y_t^*$ is the output gap. We allow time variation in the inflation gap model in (7), thus the error in the inflation equation follows stochastic volatility,

[1]Note that the limiting forecast of stationary cycle component approaches zero, so we can interpret the forecast of inflation over long horizons as approximating the trend inflation (Beveridge and Nelson, 1981).

$\lim_{j \to \infty} \mathbb{E}_t[\pi_{t+j}^g] = 0$ with probability 1.

$$\epsilon_t^{\pi} \sim N(0, e^{h_t})$$

$$\rho_t = \rho_{t-1} + \epsilon_t^{\rho} \tag{8}$$
$$\epsilon_t^{\rho} \sim TN(-\rho_{t-1}, 1-\rho; 0, \sigma_{\rho}^2)$$

Inflation gap persistence ρ_t is used for measuring the credibility of the central bank, as the rate at which convergence to the long-run target happens. This convergence depends on the monetary policy and the expectations of the private agents (Cogley, Primiceri and Sargent, 2010). Inflation gap has an $AR(1)$ process to capture the inflation gap persistence. This is unlike the persistence captured by the lagged accelerationist Phillips curve, where changes in inflation are mechanically captured by the permanent component of inflation. Here the permanant component only capture the shocks to trend inflation and the additive feature of the UC model provides a neat decomposition of the permanent and transitory shocks. We allow the persistence parameter ρ to be time-varying to capture the different degree of credibility accross different monetary regimes. Thus we allow the inflation-gap persistence parameter ρ_t to follow also a random walk process,

ρ_t has been bounded between $[0 < \rho_t < 1]$, with $\rho_t \to 1$ showing low credible central bank whereas $\rho_t \to 0$ shows a highly credible central bank.

$$\lambda_t = \lambda_{t-1} + \epsilon_t^{\lambda} \tag{9}$$
$$\epsilon_t^{\lambda} \sim TN(-\lambda_{t-1}, 1-\lambda_{t-1}; 0, \sigma_{\lambda}^2)$$

Slope of the Phillips curve shows the evolving response of the inflation gap accross years to capture the short-run dynamics of inflation and output and also to capture the changes in excess demand factors on inflation. We want to know whether the slope of the Phillips curve has become flatter in these emerging economies. There will be periods when the slope of the Phillips curve will be flatter and years when the slope of the Phillips curve is more responsive. To model such a scenario we allow the slope of the Phillips curve to evolve as a random walk process to capture changes accross years.

Note (7) nests a hybrid New Keynesian Phillips curve (NKPC) as trend inflation captures backward price setting behaviour and can also be regarded as forward looking. Backward price setting dynamics is nested in the trend component which can be shown as $\pi_t^* = \mathbf{E_{t-1}}(\pi_t^*)$, which is the weighted average of past observations (Harvey, 2014). Whereas forward looking behavior is based on (3),

$$\lim_{j \to \infty} \mathbb{E}_t[\pi_{t+j}] = \mathbb{E}_t[\pi_{t+j}^*] = \pi_t^*$$

In (9) we have the Phillips curve in gap form which can be considered as the difference between actual inflation and central bank's long-run target[2]. It has three components, inflation-gap persistence, output gap and heterogenous supply shock.

3 Data and Estimation

3.1 Data

We study six large emerging economies : Brazil, Chile, India, Indonesia, Mexico and South Africa. All CPI and real GDP series has been obtained from Fred database and in some cases from the respective central bank websites. Below are data sample periods.

Table 1: Data sample period

Country	Sample period
Brazil	1996Q3 : 2023Q3
Chile	1996Q3 : 2023Q3
India	1996Q3 : 2023Q2
Indonesia	2000Q3 : 2025Q1
Mexico	1993Q3 : 2024Q2
South Africa	1993Q3 : 2024Q3

CPI inflation is measured as annualized quarterly inflation, $(400 * log(p_t/p_{t-1})$. The domestic output gap is defined as deviation of 100 times log of real GDP from its model implied trend.

3.2 Estimation

We estimate the bivariate UC model in a fully Bayesian manner using Markov Chain Monte Carlo (MCMC) methods. Instead of Kalman-filter-based state simulation, we employ precision samplers that exploit band-matrix routines to draw state vectors efficiently, an approach that is computationally faster and scales well with sample length. Full details of the sampler and the algebra of the posterior updates are provided in the Appendix.

Stochastic volatility in the inflation gap and trend blocks is handled with the Kim–Shephard–Chib (KSC) auxiliary mixture approximation, which allows conditionally Gaussian state updates within the precision-sampling framework. The Appendix describes the mixture-indicator draws and the resulting Gaussian forms used for the g_t and h_t volatility states.

[2]Constructing the inflation gap as the deviation of inflation from a slowly evolving trend has been shown to improve forecasting performance relative to using raw inflation alone (Faust and Wright, 2013).

3.3 Priors and initialization

Priors are standard, weakly informative inverse-gamma distributions for variance parameters and Gaussian priors for initial states and static coefficients (including $\Gamma=(y_0^*, y_{-1}^*)$). Initial conditions for the volatility and level states $g_1, h_1, \pi_1^*, y_1^*, \lambda_1, \rho_{\pi,1}$ are set with diffuse normal priors. Hyperparameter values and the complete prior list are summarized in the Appendix.

Posterior simulation proceeds by alternating Gibbs and tailored Metropolis–Hastings steps across blocks: (i) volatility states via KSC mixture updates, (ii) trend and gap states via precision sampling, and (iii) time-varying Phillips-curve parameters including bounded random-walk processes for λ_t and $\rho_{\pi,t}$ with truncated-normal innovations.

The Appendix provides the block-wise conditional posteriors and linear-algebra primitives used in each draw.

4 Results

4.1 Trend inflation

Figure 1: Trend and Actual Inflation

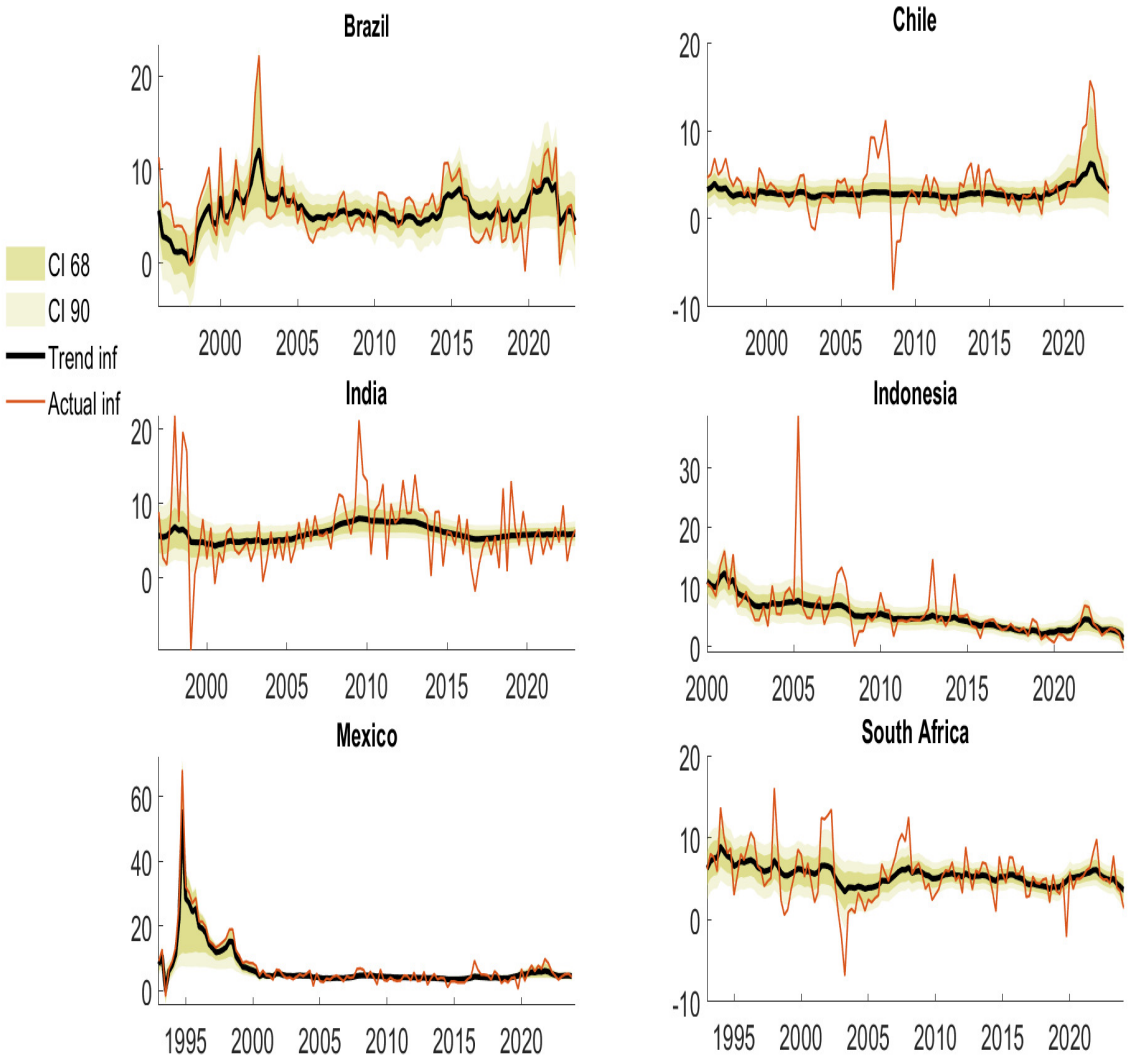

Notes: The figure plots the median of the posterior distribution of the time-varying trend inflation and actual inflation. The shaded areas denote the 68% and 90% credible intervals.

Figure 1 plots the median estimates of time-varying trend inflation alongside actual inflation for the six emerging economies in the sample. The trend estimates are generally precise, with wider credible intervals only during the COVID-19 period for Brazil and Chile, reflecting heightened macroeconomic uncertainty at that time. A key finding is the

substantial reduction in trend inflation over time, particularly in countries that adopted inflation targeting (IT) early in the sample

Indonesia, Mexico, and South Africa exhibit marked declines in trend inflation relative to the early years. For instance, Indonesia's average trend inflation fell from around 8.8 percent in the pre-IT period (2000–2005) to 4.3 percent during the IT years (2006–2024). Mexico shows an even sharper improvement: trend inflation averaged 14.7 percent before IT adoption (1993–2000) but dropped to 4.3 percent thereafter. These declines suggest that IT frameworks were effective in re-anchoring long-term expectations in these economies. India's experience is more muted. Trend inflation fell only slightly from 6.2 percent in the pre-IT period (1996–2015) to 5.5 percent after IT adoption in 2016. Chile displays persistently low trend inflation of about 3 percent over the entire sample, indicative of its early and credible monetary policy framework. Brazil, in contrast, maintains a relatively high trend inflation (5–6 percent), showing limited progress in anchoring inflation expectations despite having adopted IT in 1999. Another striking feature of Figure 1 is the persistent divergence between actual and trend inflation in most economies (except Mexico). This highlights the importance of cyclical factors, the inflation gap in explaining short-run inflation fluctuations as demonstrated in Section 5. For policymakers, this suggests that managing the inflation gap through countercyclical policy remains crucial, even as the trend component provides a long-run anchor.

4.1.1 Volatility of Trend Inflation and Inflation Gap

Figure 2 shows the standard deviation of shocks to trend inflation, which can be considered as a proxy for the degree of anchoring of long-term inflation expectations. A lower standard deviation indicates greater stability and stronger anchoring. We document a pronounced downward trajectory in the volatility of trend inflation shocks for India, Indonesia, Mexico, and South Africa. The improvement is most striking for Mexico, where posterior standard deviation declines from 10.1 in the pre-IT period to just 0.3 in the most recent phase, consistent with a highly credible inflation targeting regime. Similarly, South Africa and Indonesia show gradual but meaningful declines, consistent with improved policy frameworks over time. Brazil and Chile also experience some reduction in trend inflation volatility, but both display a temporary spike during the COVID-19 pandemic, reflecting a deterioration in the predictability of long-run inflation.

For Brazil in particular, the volatility remains relatively elevated throughout the sample, with wide posterior intervals indicating high uncertainty. This is consistent with survey and market-based evidence suggesting that long-term expectations are less firmly anchored in Brazil than in Chile or Mexico (Pooter et al., 2014; IMF, 2012). The deterioration coincides with major macroeconomic disruptions global commodity shocks and domestic monetary tightening which contributed to a sharp slowdown in Brazilian GDP growth from 7.5 percent in 2010 to just 2.7 percent in 2011.

Figure 2: Standard Dev. of Shocks to Trend Inflation

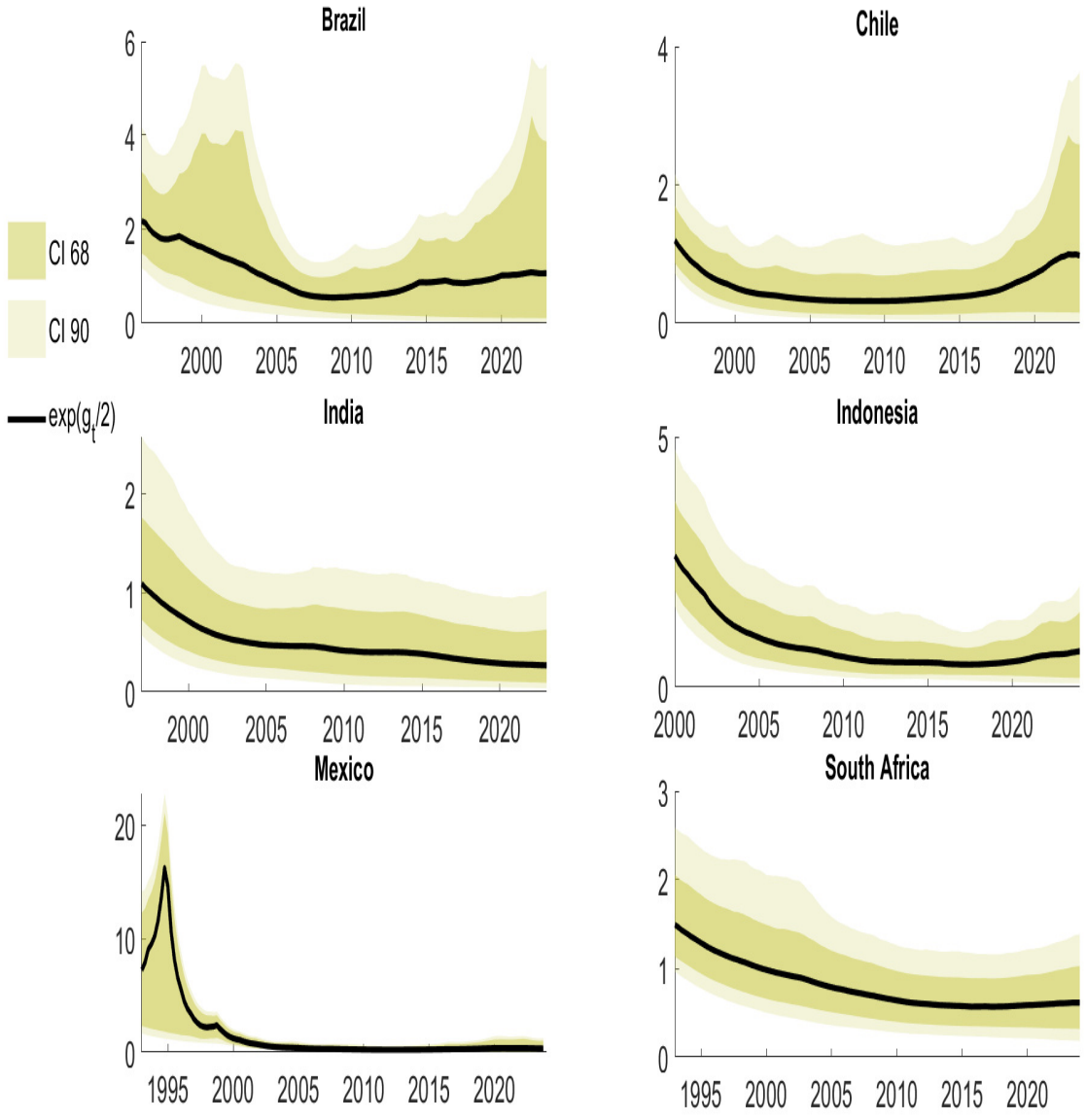

Notes: The figure plots the posterior distribution of the standard deviation of shocks to trend inflation. Shaded areas denote the 68% and 90% credible intervals.

Figure 3 further reveals that the volatility of the inflation gap is substantial in the early years for Brazil, India, and South Africa, indicating greater cyclical instability. For South Africa, the volatility of the inflation gap has declined steadily over time, suggesting improved stabilization policy. By contrast, Brazil continues to display relatively high volatil-

ity, and during COVID-19 both Brazil and Chile experienced pronounced spikes underscoring their vulnerability to large supply and demand shocks.

Figure 3: Standard Dev. of Shocks to Inflation Gap

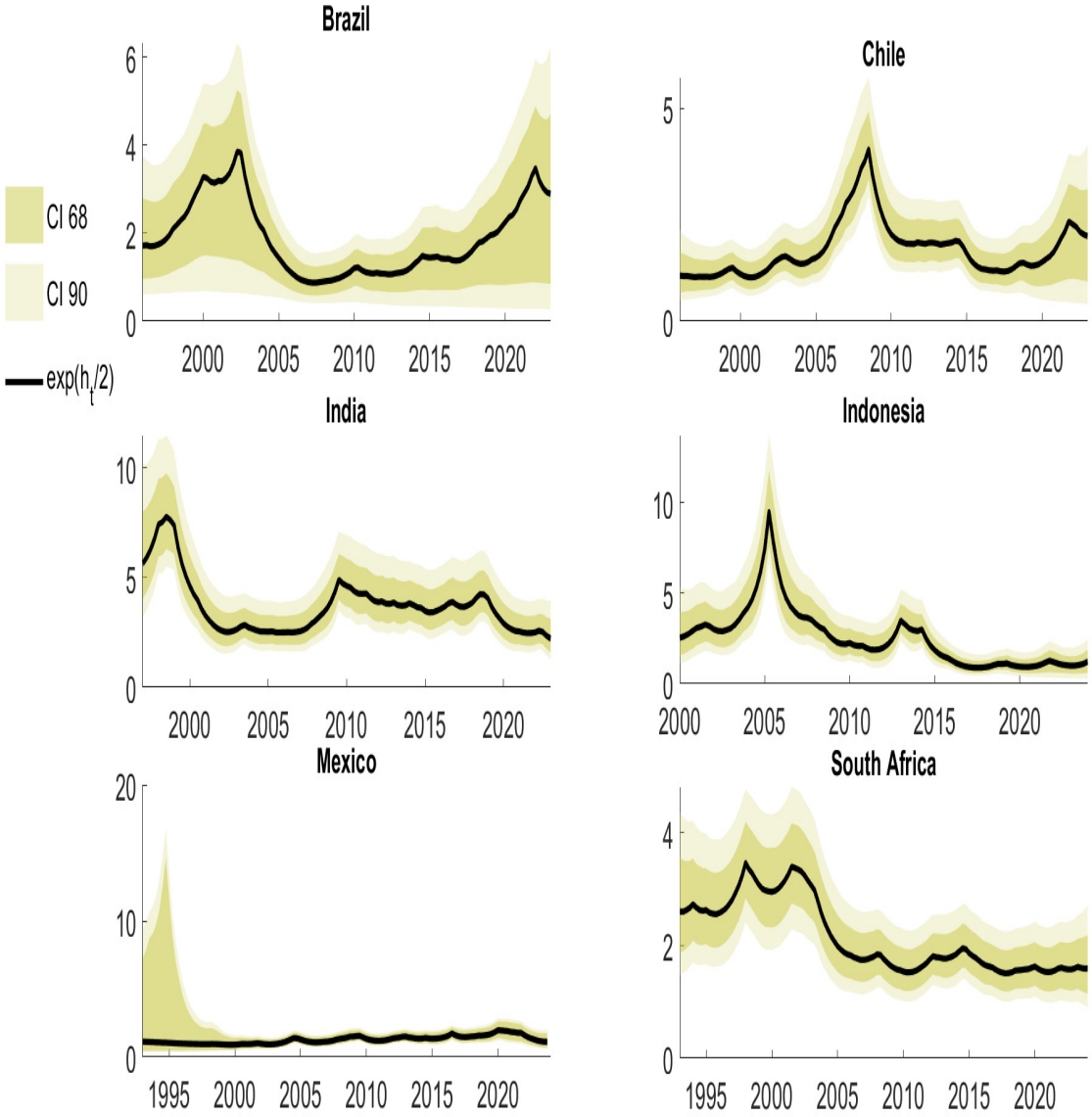

Notes: The figure plots the posterior distribution of the standard deviation of shocks to the inflation gap. Shaded areas denote the 68% and 90% credible intervals.

Overall, Figures 1–3 provide strong evidence that IT adoption has been associated with (i) lower trend inflation, (ii) better anchoring of inflation expectations (via lower volatility of trend shocks), and (iii) and in some cases, reduced cyclical volatility. While Brazil remains an exception on several margins.

4.2 Trend Output and Output Gap

Figure 4 presents the posterior estimates of trend output along with actual output (log real GDP) for the six emerging economies. The model tracks the underlying growth path while filtering out short-run fluctuations. For most economies, the posterior credible intervals around trend output are narrow, indicating precise identification of the long run component. The exception is Indonesia, where wider intervals point to greater uncertainty in distinguishing between trend and cyclical movements, likely reflecting both data limitations and the relatively shorter sample period available.

The reliability of output gap estimates has been widely debated, particularly for emerging economies, and even in advanced economies their robustness remains contentious (Orphanides & Van Norden, 2002; Jarociński & Lenza, 2018). Nevertheless, our model produces economically meaningful and internally consistent output gap measures that align well with major global and domestic business cycle episodes. Figure 5 shows the resulting estimates of the output gap, the deviation of actual output from its time-varying trend. Three patterns stand out.

First, gaps turn sharply negative across all countries during major global shocks. The dot-com collapse (2000–2002) generated negative gaps in every country, consistent with the transmission of external demand shocks to emerging markets. The global financial crisis (2008–2009) produced even larger and more synchronized contractions, with steep declines in industrial production and exports in Brazil, Mexico, and South Africa. India had experienced a dramatic swing in export growth from positive 40 percent to negative 22 percent within two quarters, leading to a sharp output gap contraction.

Second, the COVID-19 pandemic triggered the most severe output contractions in the sample period. All six economies experienced unprecedented drops in activity, but the speed of recovery has been highly uneven. Chile rebounded relatively quickly, with its output gap turning positive by 2022, helped by robust fiscal support, accommodative monetary policy, and favorable external demand for commodities. By contrast, India and Indonesia still exhibit negative output gaps in the post-COVID period, suggesting a slower recovery constrained by domestic demand weaknesses, labor market disruptions, and slower re-integration into global supply chains.

A notable feature of Figure 5 is the asymmetry between downturns and recoveries. While crises generate deep and rapid negative gaps, the subsequent recoveries are typically more gradual and heterogeneous across countries. This asymmetry points to structural vulnerabilities of emerging economies, including reliance on external demand, procyclical fiscal policy, and limited automatic stabilizers.

Figure 4: Trend and Actual Output

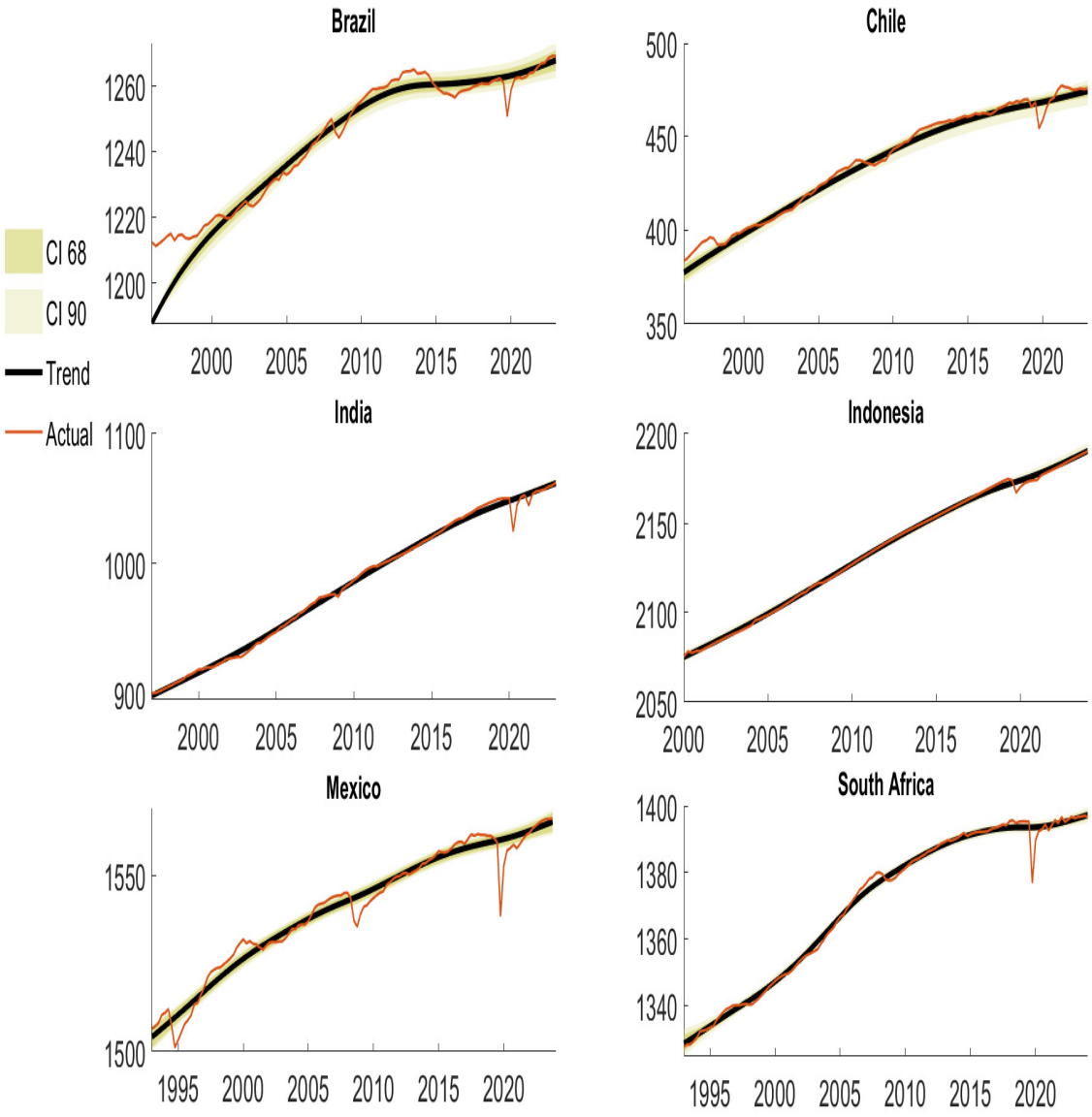

Notes: The figure plots the median posterior estimates of trend output and log of RGDP. The shaded areas denote the 68% and 90% credible intervals.

Persistent negative output gaps in India and Indonesia imply weak demand-side pressures, which may have limited the effectiveness of recent monetary tightening in curbing inflation. In contrast, Chile and South Africa saw a quicker closure of output gaps, suggesting that demand-side factors contributed more strongly to recent inflation surges, making monetary policy transmission more effective. Taken together, Figures 4 and 5 emphasize that understanding inflation dynamics in emerging economies requires careful modeling of the output gap, as global shocks produce common cyclical patterns but domestic structural factors shape recovery paths.

Figure 5: Output Gap

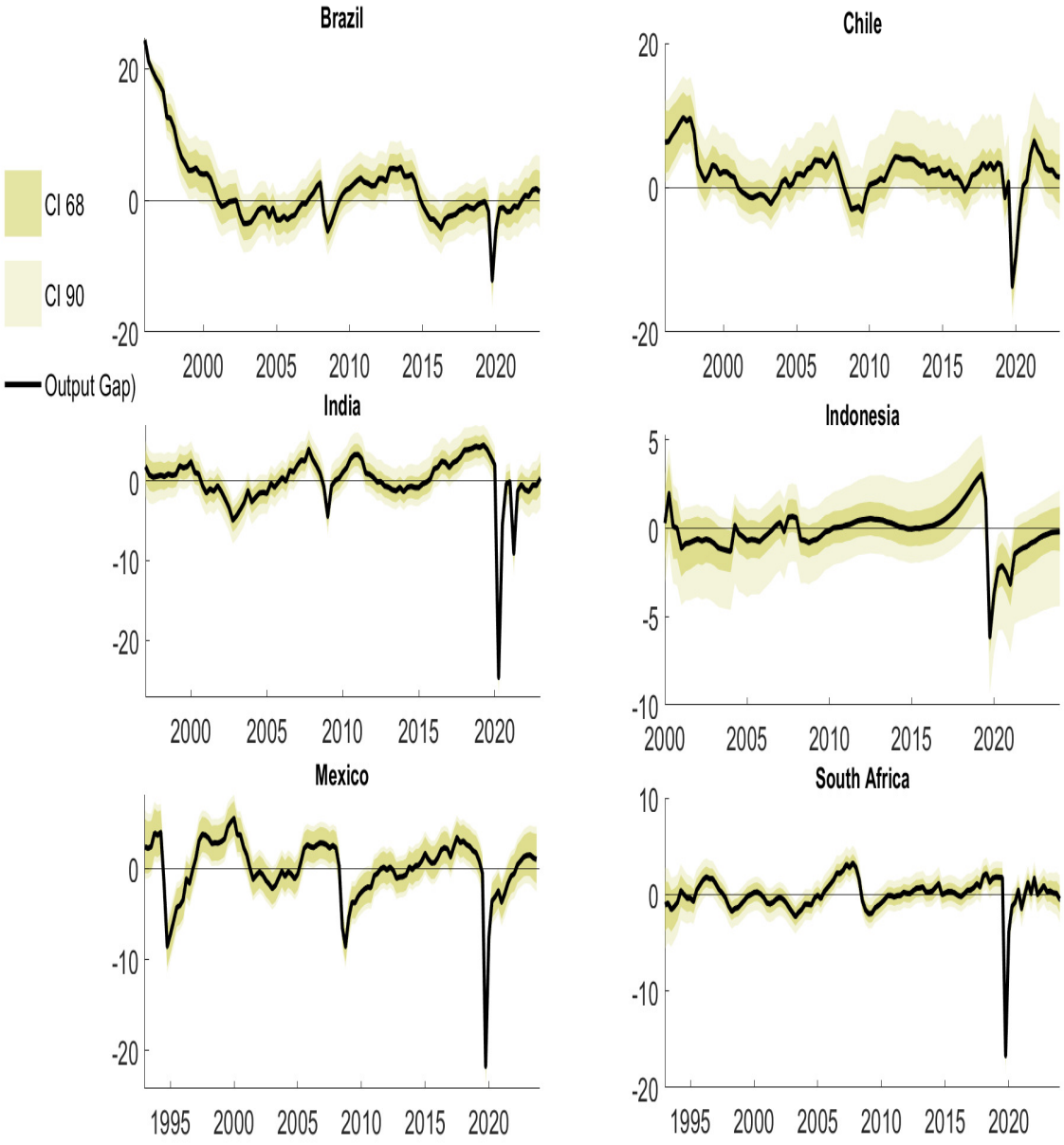

Notes: The figures plot the median posterior estimates of the output gap, which is the difference between GDP growth rate (annualized) and posterior distribution of the trend output. The shaded areas denote the 68% and 90% credible intervals.

4.3 Time-varying Phillips curve slope estimates

Figure 6: Time-varying Slope of the Phillips Curve

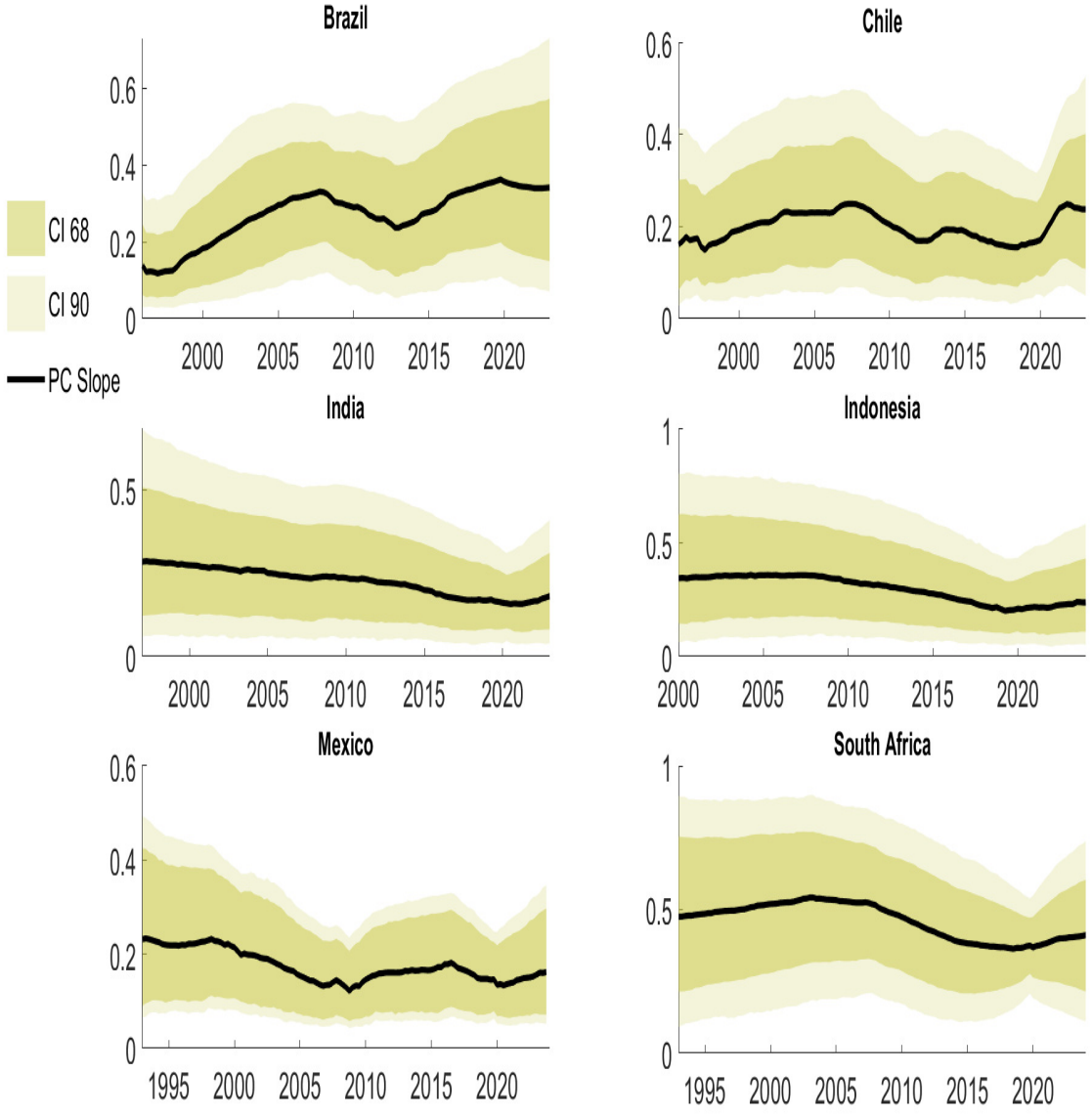

Notes: The figures plot the median estimates of the posterior distribution of the time-varying slope of the Phillips curve. The shaded areas denote the 68% and 90% credible intervals.

Models with a time-invariant Phillips curve slope fail to capture the evolving nature of the inflation–output trade-off and often deliver poor forecasting performance. This motivates the use of time-varying parameter models that allow the slope to adjust over time. Figure 6 reports the estimated time-varying Phillips curve slopes for the sample economies. Chile and Mexico exhibit relatively flat slopes throughout the period, indi-

cating a weak response of inflation to domestic demand conditions. By contrast, Brazil and South Africa display steeper and more volatile slopes, with Brazil's estimates ranging between 0.11 and 0.35 and South Africa's between 0.35 and 0.53, suggesting that inflation in these economies is more sensitive to output fluctuations.

India shows a particularly interesting pattern, the Phillips curve slope declines sharply after the adoption of inflation targeting. The median estimate falls from around 2.4 during the pre-IT period (1997–2015) to about 0.15 in the IT years, implying a significant flattening of the Phillips curve and weaker pass-through from the output gap to inflation. This result helps explain why inflation remained elevated despite negative output gaps during COVID-19, as demand-side pressures played a smaller role in price dynamics. Taken together, these findings underscore the importance of allowing for time variation in the Phillips curve slope. Fixed-slope models would fail to capture episodes where inflation became either highly sensitive or largely unresponsive to economic slack, potentially leading to misguided policy conclusions.

4.4 Inflation Gap Persistence

Figure 7 plots the time-varying estimates of inflation gap persistence for all six countries. Inflation gap persistence captures the speed with which inflation converges to the central bank's long-run target (Cogley et al., 2010) and can therefore be interpreted as a measure of monetary policy credibility. A value close to zero indicates that inflation quickly reverts to target—signaling high credibility whereas a value closer to one suggests weak credibility and slow convergence. Our results reveal substantial cross-country heterogeneity and time variation.

Inflation gap persistence rises in South Africa sharply in the early 2000s, indicating a deterioration of central bank credibility during this period. This is consistent with the 2002 rand depreciation crisis, which temporarily destabilized expectations. After 2005, persistence declines markedly from around 0.5 to 0.15 suggesting improved credibility and faster convergence of inflation to target. This improvement is consistent with Kabundi and Mlachila (2019), who report that exchange rate pass-through to CPI inflation declined after 2007. A mild uptick is observed during COVID-19, likely reflecting heightened uncertainty, but credibility remains stronger than in the early 2000s.

Brazil's experience is more concerning. After adopting inflation targeting in 1999 during a currency crisis, inflation gap persistence remained relatively stable between 2004 and 2010 but increased sharply from 2011 onward, peaking during the 2015–2016 recession. These results suggest that repeated external shocks and macroeconomic instability undermined the credibility of Brazil's inflation targeting regime during the later part of the sample.

Figure 7: Inflation Gap Persistence

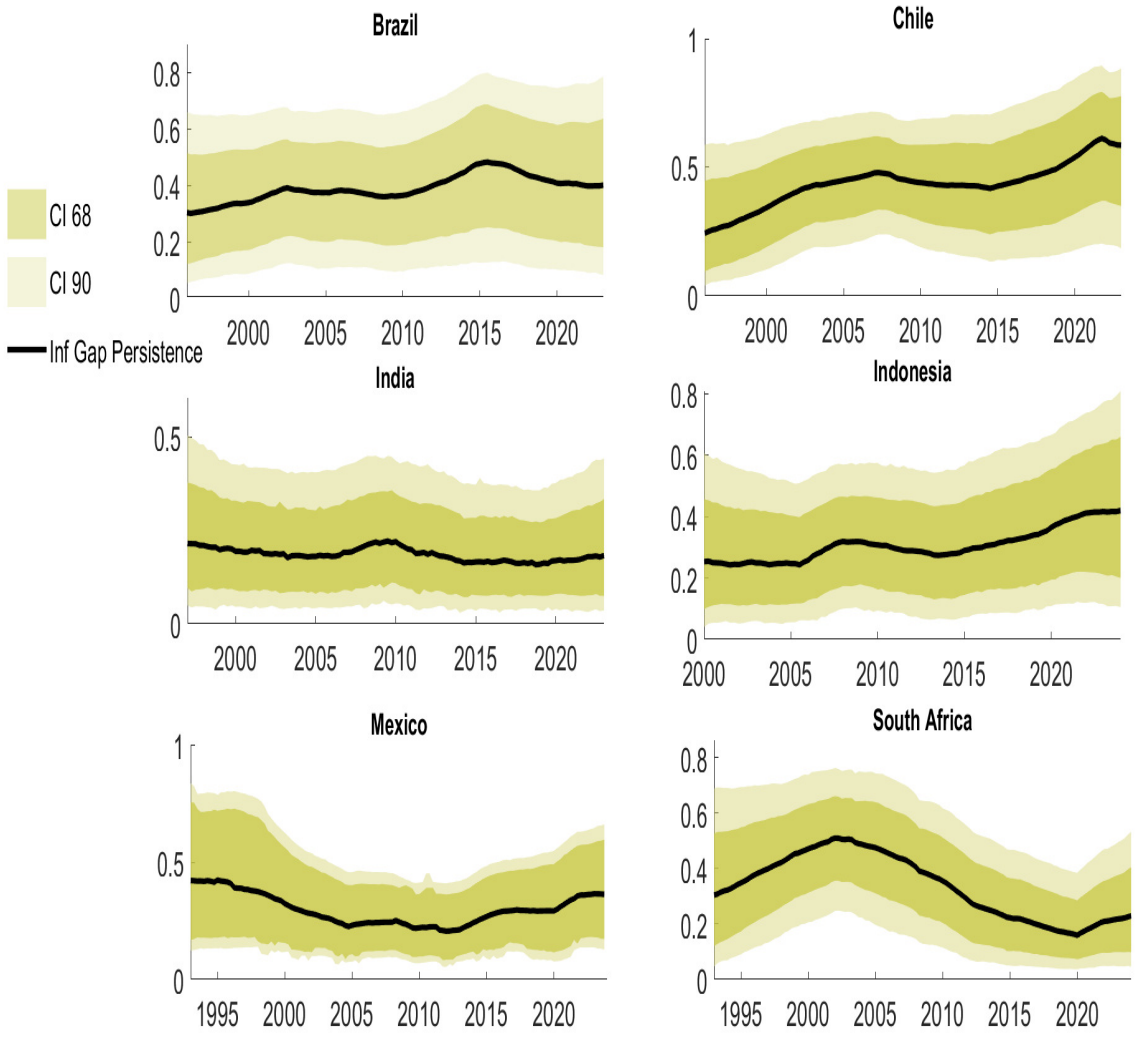

Notes: The figures plot the median estimates of the posterior distribution of the time-varying inflation gap persistence parameter. The shaded areas denote the 68% and 90% credible intervals.

India stands out for having persistently low inflation gap persistence—around 0.2—implying relatively strong credibility of monetary policy. A small hump appears during the 2008–2009 global financial crisis, reflecting a temporary decline in credibility due to global shocks. Interestingly, the introduction of formal inflation targeting in 2016 does not lead to a significant change in persistence, nor do we observe notable changes during the COVID-19 years, suggesting that credibility remained broadly stable throughout.

Overall, these results highlight that while some emerging economies, such as South Africa, have strengthened their monetary credibility over time, others like Brazil have faced challenges in maintaining firmly anchored inflation expectations, particularly during periods of macroeconomic stress.

Indonesia adopted inflation targeting in 2005. We notice that inflation gap persistence

for Indonesia has been lower than Brazil and Chile around 0.3-0.5 band, but it has remained elevated. During COVID-19 there is a sharp increase showing much reduced credibility. Thus we don't find better credibility in the conduct of monetary policy from the inflation gap persistence for Indonesia.

Central bank of Chile introduced inflation targeting in 1999. In the case of Chile we notice quite volatile inflation gap persistence showing not much improvement in the central bank credibility after introduction of inflation targeting.

5 Contributions of Trend inflation and Inflation Gap to Inflation Variation

5.1 Trend share

To quantify the relative importance of trend inflation and the inflation gap in driving observed inflation dynamics, we follow Morley, Piger and Rasche (2015) and construct time-varying variance decomposition of multi quarter changes in inflation.

Recall that inflation is decomposed as

$$\pi_t = \pi_t^* + \pi_t^g$$

For each country and each posterior draw of the parameters and states, we consider the $j - quarter$ change in inflation,

$$\Delta^j \pi_t = \pi_t - \pi_{t-j}, \quad j \in \{2,4,12\}$$

correspnding to 2, 4 and 12 quarter inflation changes. Under the unobserved components structure, shocks to trend inflation and to the inflation gap are orthogonal, so the variance of $\Delta^j \pi_t$ can be written as,

$$Var(\Delta^j \pi_t) = Var(\Delta^j \pi_t^*) + Var(\Delta^j \pi_t^g)$$

As trend inflation follows a driftless random walk with stochastic volatility, so the variance of $j - quarter$ change in trend inflation is simply the sum of the time-varying innovation variances over the relevant window,

$$Var(\Delta^j \pi_t^*) = \sum_{s=t-j+1}^{t} \sigma_{v,s}^2$$

The variance of the corresponding change in the inflation gap, $\Delta^j \pi_t$, is obtained from the covariance recursion for the gap implied by the estimated states and parameters. We summarize the time-varying share of the variance of $\Delta^j \pi_t$ due to trend inflation, for each t and horizon j by ,

$$V_{\pi,t}^*(j) = \frac{Var(\Delta^j \pi_t^*)}{Var(\Delta^j \pi_t^*) + Var(\Delta^j g_t)}$$

We compute $V^*_{\pi,t}(j)$ for every retained posterior draw and summarise the distribution at each date using the posterior median. The contribution of the inflation gap to the variance of $j-quarter$ changes in inflation is the complementary share,

$$V^g_{\pi,t}(j) = 1 - V^*_{\pi,t}(j)$$

In figure 8, we show the posterior median of the contribution of the trend inflation and inflation gap to the variation in inflation for all the six countries.

Figure 8: **Variance Decomposition: Contribution of Trend Inflation vs Inflation Gap**

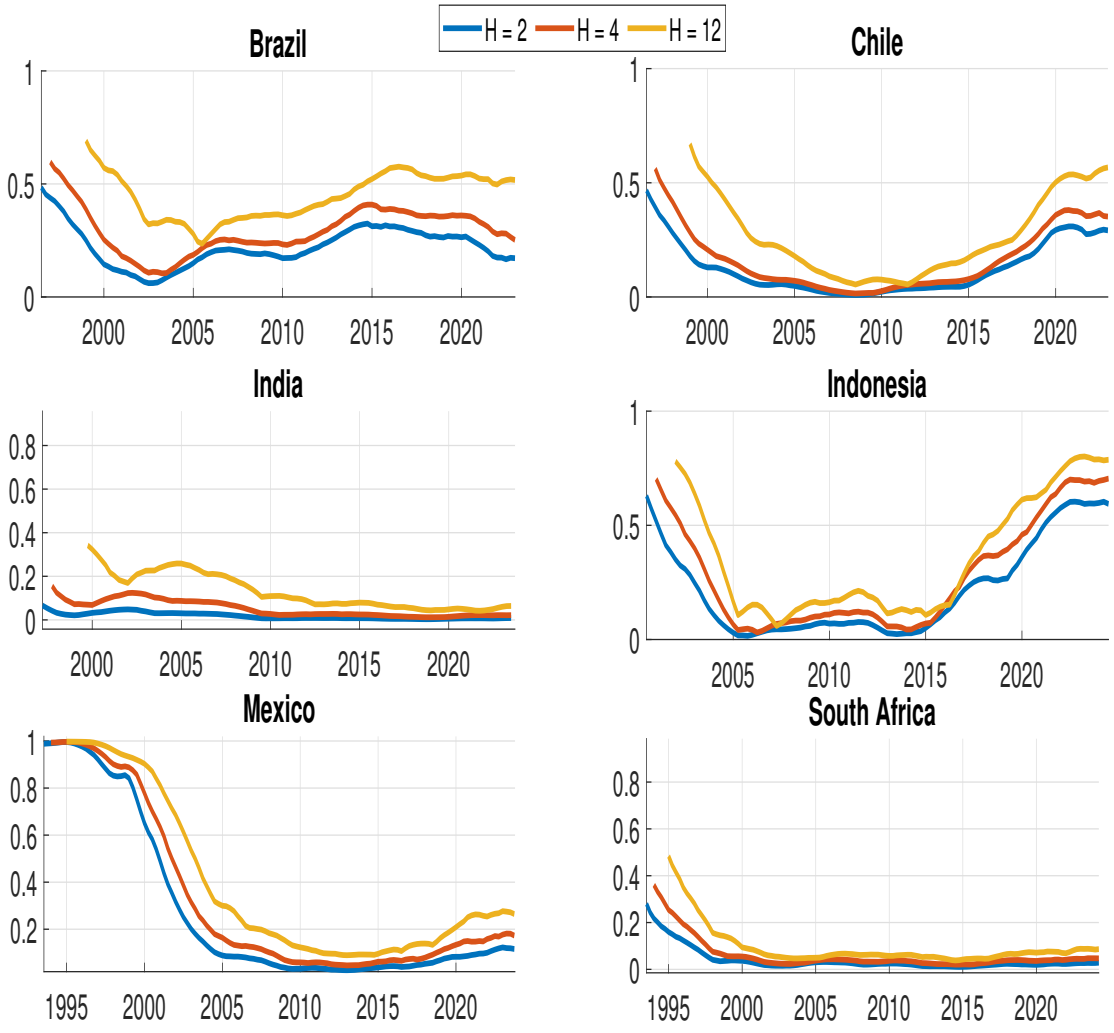

Notes: Contribution of trend inflation to the variance of inflation. The figure reports the median posterior estimates of the share of inflation variance that is explained by the variance of changes in trend inflation across different forecast horizons.

Figure 8 presents the variance decomposition of inflation changes, highlighting the relative importance of trend inflation versus the inflation gap. A fundamental property

of the model is that the contribution of trend inflation tends to increase with the forecast horizon; this is expected given that the trend is specified as a unit root process, which naturally dominates the variance of inflation changes as the horizon grows.

However, the results reveal significant cross-country heterogeneity, particularly in the early part of the sample. For Brazil and Chile, the contribution of trend inflation is notably high, ranging between 0.5 and 0.6, whereas for India and South Africa, the variation in inflation is predominantly driven by the inflation gap. This distinction is critical for evaluating monetary policy effectiveness. Since trend inflation captures the permanent component of inflation, it is intrinsically linked to long-horizon inflation expectations. Consequently, when inflation changes at medium-term horizons (two to three years) are driven by the transitory component rather than the trend, it serves as evidence that inflation expectations are anchored.

Applying this framework to the latter half of the sample reveals diverging degrees of anchoring. For India and Mexico (post-2010) and South Africa (post-2005), inflation changes at the three-year horizon are increasingly dominated by the transitory component, signaling a successful anchoring of expectations. In contrast, Brazil, Chile, and Indonesia exhibit a persistently higher contribution from the trend inflation component. This dominance of the permanent component suggests a lower degree of expectation anchoring, implying that the respective central banks have been less successful in minimizing the propagation of permanent inflation shocks through monetary policy.

5.2 Output-gap and Residual contributions to the Inflation Gap

In this section, we examine through variance decomposition what drives fluctuations in the inflation gap. We decompose the variance of inflation gap into contributions from shocks to the output gap and residual shocks specific to the Phillips curve. Conditional on the estimated paths of the time-varying persistence ρ_t and λ_t,we write the joint dynamics of the output gap and inflation gap in companion form and run three covariance recursions : one with both shocks active, one with only output gap shocks, and one with only Phillips curve residual shocks. This yields time-varying variance components $Var_x(\pi_t^g)$ and $Var_\epsilon(\pi_t^g)$, from which we contruct the corresponding shares

$$R_{x,t} = \frac{Var_x(\pi_t^g)}{Var(\pi_t^g)} \text{ (output-gap shock share)}$$

$$R_{\epsilon,t} = \frac{Var_\epsilon(\pi_t^g)}{Var(\pi_t^g)} \text{(inflation residual shock share)}$$

again summarized by posterior medians.

Figure 9: Contribution of output gap

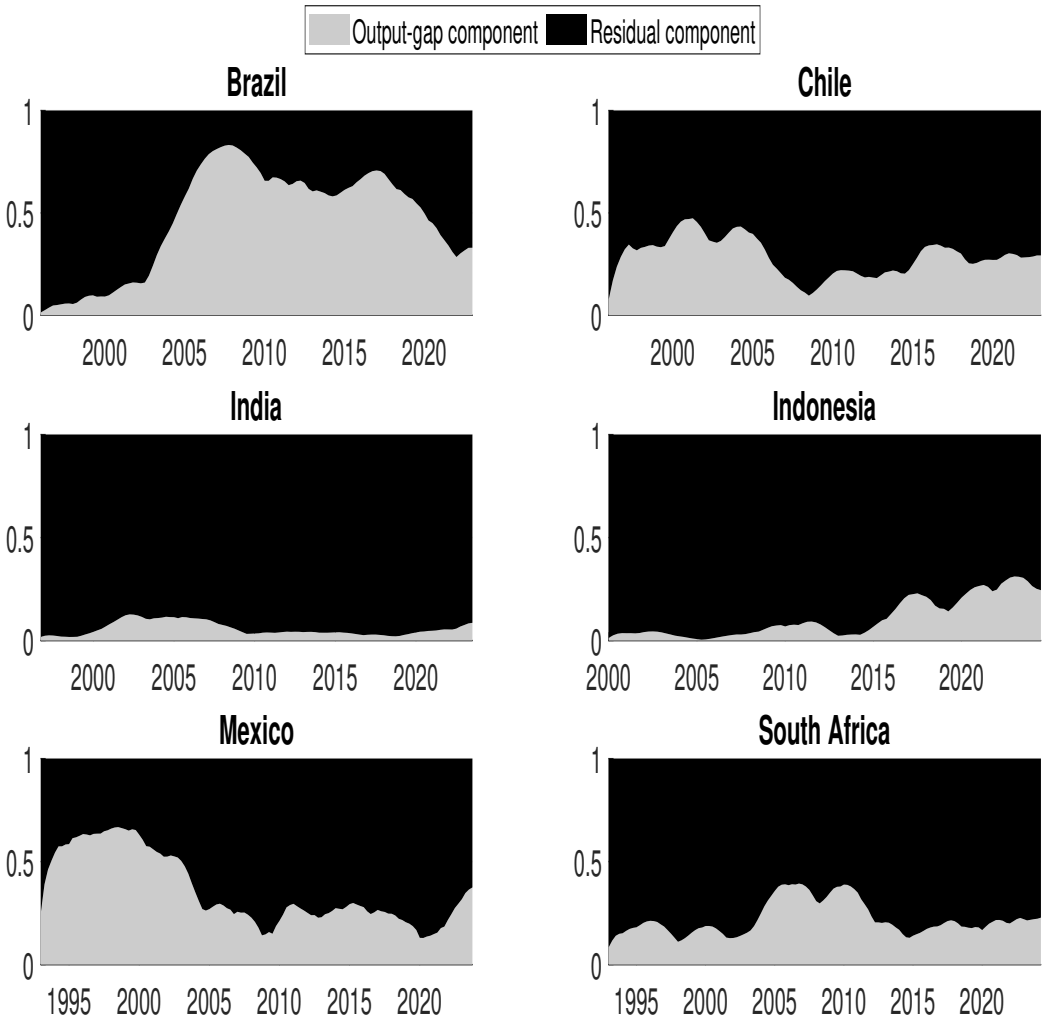

Notes: Contribution of the output gap and the residual component to the variance of the inflation gap. The figure reports the median posterior estimates of the share of the inflation gap variance explained by the output gap and the residual component

For the majority of the countries, the residual component (black area) is the overwhelming driver of the inflation gap, implying that transitory inflation fluctuations are largely disconnected from domestic demand conditions. For India and Indonesia, the output-gap contribution (light grey area) is negligible throughout the sample. This suggests that cyclical inflation in these countries is almost entirely driven by supply-side factors rather than excess demand. South Africa shows a similar pattern where the residual component dominates, with the output gap making only minor contributions, notably around 2005–2010. For Chile, the output gap has a moderate but limited role (appearing to explain roughly 20–30% of variance), with residuals still being the primary driver.

Brazil stands out as the unique exception in the sample. The output-gap component (light grey area) is substantial, often exceeding 50% of the variance between 2005 and 2020. This indicates that unlike its peers, Brazil's transitory inflation is highly sensitive to the business cycle and domestic demand shocks. This aligns with earlier findings in the paper that Brazil has a steep Phillips curve slope. Mexico exhibits a regime shift. In the early sample (pre-2000), the output gap contributed significantly (>50%) to inflation gap volatility. However, this contribution collapsed in the latter half of the sample, with residuals (supply shocks) becoming dominant.

The analysis of Figure 9 suggests that for most emerging economies (India, Indonesia, South Africa), the New Keynesian Phillips Curve (NKPC) mechanism—where demand drives inflation deviations—is statistically overwhelmed by "noise" or supply shocks. Brazil is the only case where the output gap is the primary structural driver of cyclical inflation variance, making it a "textbook" case of demand-pull inflation relative to the other emerging economies in the study.

6 Robustness

6.1 Prior Sensitivity

We target the priors that most directly govern the volatility of the shocks that drive our key objects, basically trend inflation and inflation gap. In unobserved components models with stochastic volatility, the parameters that govern how much h_t and g_t can move are the ones likely to be weakly identified near zero and therefore most prior leveraged. It thus becomes important to know how the innovation variation of these state variables is sensitive to the choice of the priors. Thus we perturb the priors on the random walk variance of h_t and g_t.

In each country's MCMC run, we scale the inverse-gamma hyperparameters on the stochastic volatility variances $\sigma_h^2 \sim \text{IG}(\nu_h, S_h)$ and $\sigma_g^2 \sim \text{IG}(\nu_g, S_g)$. We re-estimate the model under the ladder of scaled prior scales, where $S_{h_0} = 0.1(\nu_{h_0} - 1)$ and $S_{g_0} = 0.1(\nu_{g_0} - 1)$ are scaled by $\kappa S_{h_0}, \kappa S_{g_0}$ with $\kappa \in \{0.5, 1, 1.5, 2, 2.5\}$. This makes the log-volatility paths more or less flexible a priori without changing the likelihood or state evolution. [figure to the added in the appendix]

7 Conclusion

This paper has examined inflation dynamics in six large emerging economies through a time-varying Phillips curve framework with stochastic trend and cyclical components. By decomposing inflation into its persistent and transitory drivers, we uncover several important insights.

First, inflation targeting has generally been successful in reducing trend inflation and improving the anchoring of expectations, particularly in Mexico, Indonesia, and South Africa. Brazil stands out as an exception, with weakly anchored expectations and high volatility in trend inflation even after adopting inflation targeting.

Second, the cyclical component of inflation remains highly relevant for most countries, with output gaps turning sharply negative during major global shocks such as the Global Financial Crisis and COVID-19. Post-COVID recoveries, however, have been uneven across economies, with Chile showing stronger convergence than India and Indonesia, where negative output gaps persist.

Third, we find substantial heterogeneity in the slope of the Phillips curve: while Chile, Mexico, and post-2015 India exhibit relatively flat slopes, Brazil and South Africa show steeper and more volatile responses of inflation to the output gap. These differences underscore the importance of allowing for time variation in the Phillips curve slope to capture evolving inflation-output tradeoffs.

Fourth, our results on inflation gap persistence provide new evidence on central bank credibility. While India and post-2005 South Africa display relatively strong credibility with low persistence, Brazil, Chile, and Indonesia continue to experience higher or more volatile persistence, reflecting weaker anchoring of expectations.

Finally, variance decompositions provide a more granular view of anchoring and structural drivers. While trend inflation historically drove variation in Mexico, our results show a successful regime shift, with the transitory component dominating in the post-IT period. In contrast, Brazil remains an outlier where permanent trend shocks continue to drive a significant share of inflation variation. Crucially, we uncover a divergence in recent years: while the inflation gap remains the dominant driver in India and South Africa, we observe a concerning rise in the contribution of trend inflation in Chile and Indonesia, signaling potential risks to expectation anchoring in the post-COVID period. Furthermore, decomposing the cyclical component reveals a stark structural divide. Brazil emerges as the unique case where domestic output gaps (demand pressures) explain the majority of cyclical fluctuation, consistent with its steeper Phillips curve. In contrast, for India, Indonesia, and South Africa, cyclical inflation is overwhelmingly driven by residual supply-side factors rather than excess demand.

References

[1] Ball, L.M. and Mazumder, S., 2011. Inflation dynamics and the great recession (No. w17044). National Bureau of Economic Research.

[2] Basistha, A. and Startz, R., 2008. Measuring the NAIRU with reduced uncertainty: a multiple-indicator common-cycle approach. The Review of Economics and Statistics, 90(4), pp.805-811.

[3] Barnichon, Regis, and Geert Mesters. "The phillips multiplier." Journal of Monetary Economics 117 (2021): 689-705.

[4] Bernanke, B., 2007. Inflation expectations and inflation forecasting (No. 306). Board of Governors of the Federal Reserve System (US).

[5] Beveridge, S. and Nelson, C.R., 1981. A new approach to decomposition of economic time series into permanent and transitory components with particular attention to measurement of the 'business cycle'. Journal of Monetary economics, 7(2), pp.151-174.

[6] Blanchard, O., Cerutti, E. and Summers, L., 2015. Inflation and activity–two explorations and their monetary policy implications (No. w21726). National Bureau of Economic Research.

[7] Cecchetti, S.G., Hooper, P., Kasman, B.C., Schoenholtz, K.L. and Watson, M.W., 2007, March. Understanding the evolving inflation process. In US Monetary Policy Forum (Vol. 8, pp. 5-23).

[8] Chan, J.C. and Jeliazkov, I., 2009. Efficient simulation and integrated likelihood estimation in state space models. International Journal of Mathematical Modelling and Numerical Optimisation, 1(1-2), pp.101-120.

[9] Chan, J.C., Koop, G. and Potter, S.M., 2016. A bounded model of time variation in trend inflation, NAIRU and the Phillips curve. Journal of Applied Econometrics, 31(3), pp.551-565.

[10] Cogley, T. and Sbordone, A.M., 2008. Trend inflation, indexation, and inflation persistence in the New Keynesian Phillips curve. American Economic Review, 98(5), pp.2101-2126.

[11] Cogley, T., Primiceri, G.E. and Sargent, T.J., 2010. Inflation-gap persistence in the US. American Economic Journal: Macroeconomics, 2(1), pp.43-69.

[12] Coibion, O. and Gorodnichenko, Y., 2015. Is the Phillips curve alive and well after all? Inflation expectations and the missing disinflation. American Economic Journal: Macroeconomics, 7(1), pp.197-232.

[13] De Pooter, M., Robitaille, P., Walker, I. and Zdinak, M., 2018. Are long-term inflation expectations well anchored in Brazil, Chile, and Mexico?. 35th issue (June 2014) of the International Journal of Central Banking.

[14] Dotsey, M., Fujita, S. and Stark, T., 2018. Do Phillips curves conditionally help to forecast inflation?. 55th issue (September 2018) of the International Journal of Central Banking.

[15] Fuhrer, J.C., 1997. The (un) importance of forward-looking behavior in price specifications. Journal of Money, Credit, and Banking, pp.338-350.

[16] Gondo, R. and Yetman, J., 2018. Anchoring of inflation expectations in Latin America. Serie de.

[17] Harvey, A., 2014. Modelling the Phillips curve with unobserved components. In Perspectives on Econometrics and Applied Economics (pp. 7-18). Routledge.

[18] Jarociński, M. and Lenza, M., 2018. An inflation-predicting measure of the output gap in the euro area. Journal of Money, Credit and Banking, 50(6), pp.1189-1224.

[19] Kuttner, K.N., 1994. Estimating potential output as a latent variable. Journal of business & economic statistics, 12(3), pp.361-368.

[20] McLeay, M. and Tenreyro, S., 2020. Optimal inflation and the identification of the Phillips curve. NBER macroeconomics annual, 34(1), pp.199-255.

[21] Mishkin, F.S., 2007. Inflation dynamics. International Finance, 10(3), pp.317-334.

[22] Morley, J., Piger, J. and Rasche, R., 2015. Inflation in the G7: Mind the Gap (s)?. Macroeconomic Dynamics, 19(4), pp.883-912.

[23] Planas, C., Rossi, A. and Fiorentini, G., 2008. Bayesian analysis of the output gap. Journal of Business & Economic Statistics, 26(1), pp.18-32.

[24] Roberts, J.M., 2001. How well does the New Keynesian sticky-price model fit the data?.

[25] Stella, A. and Stock, J.H., 2013. A state-dependent model for inflation forecasting. FRB International Finance Discussion Paper, (1062).

[26] Stock, J.H. and Watson, M.W., 2007. Why has US inflation become harder to forecast?. Journal of Money, Credit and banking, 39, pp.3-33.

Appendix

A.1 Model Equations

The empirical model is a bivariate unobserved components (UC) representation linking inflation and output through a time-varying Phillips curve. The model can be summarized as:

Inflation Decomposition

The model has the following equations

$$\pi_t = \pi_t^* + \pi_t^g \tag{1a}$$

where π_t^* is trend inflation (a driftless random walk) and π_t^g is the stationary inflation gap.

Phillips curve (gap form)

$$\pi_t^g = \rho_t \pi_{t-1}^g + \lambda_t x_t + \epsilon_t^\pi \ , \quad \epsilon_t^\pi \sim N(0, e^{h_t}) \tag{2a}$$

where $x_t = y_t - y_t^*$ is the output gap, ρ_t is the time-varying persistence parameter (bounded between 0 and 1), and λ_t is the time-varying slope of the Phillips curve (also constrained to [0,1]).

Output Decomposition

$$y_t = y_t^* + x_t \tag{3a}$$

Where $x_t = y_t - y_t^*$

$$x_t = \phi_1 x_{t-1} + \phi_1 x_{t-2} + \epsilon_t^x \ , \ \epsilon_t^x \sim \mathbf{N}(\mathbf{0}, \sigma_x^2) \tag{4a}$$

The output gap follows an AR(2) to ensure identification.

Trend processes

$$\pi_t^* = \pi_{t-1}^* + \epsilon_t^{\pi^*}, \quad \epsilon_t^{\pi^*} \sim \mathbf{N}(\mathbf{0}, \mathbf{e^{g_t}}) \tag{5a}$$

$$\Delta y_t^* = \Delta y_{t-1}^* + \epsilon_t^{y^*}, \quad \epsilon_t^{y^*} \sim \mathbf{N}(\mathbf{0}, \sigma_{y^*}^2) \tag{6a}$$

State evolution for time-varying parameters

$$\rho_t = \rho_{t-1} + \epsilon_t^\rho \tag{7a}$$

$$\epsilon_t^\rho \sim TN(-\rho_{t-1}, 1 - \rho_{t-1}; 0, \sigma_\rho^2) \tag{8a}$$

$$\lambda_t = \lambda_{t-1} + \epsilon_t^\lambda \tag{9a}$$

$$\epsilon_t^\lambda \sim TN(-\lambda_{t-1}, 1 - \lambda_{t-1}; 0, \sigma_\lambda^2) \tag{10a}$$

Stochastic volatility processes

$$h_t = h_{t-1} + \epsilon_t^h \tag{11a}$$

$$\epsilon_t^h \sim \mathbf{N}(\mathbf{0}, \sigma_h^2) \tag{12a}$$

$$g_t = g_{t-1} + \epsilon_t^g \tag{13a}$$

$$\epsilon_t^g \sim \mathbf{N}(\mathbf{0}, \sigma_g^2) \tag{14a}$$

A.2 Priors and Initial Conditions

We initialize the state equations in the following manner,

$$g_1 \sim \mathbf{N}(\mu_g, V_g) \tag{15a}$$

$$h_1 \sim \mathbf{N}(\mu_h, V_h) \tag{16a}$$

$$(\pi_1^* | \mathbf{g_1}) \sim \mathbf{N}(\mu_{\pi^*}, V_{\pi^*}) \tag{17a}$$

$$y_1^* \sim \mathbf{N}(\mu_{y^*}, V_{y^*}) \tag{18a}$$

$$\lambda_1 \sim \mathbf{N}(\mu_\lambda, V_\lambda) \tag{19a}$$

$$\rho_1 \sim \mathbf{N}(\mu_\rho, V_\rho) \tag{20a}$$

$$\Gamma \sim N(\Gamma_0, V_\Gamma) \tag{21a}$$

Variance Priors

$$\sigma_x^2 \sim \mathbf{IG}(\underline{\nu}_x, \underline{S}_x) \tag{22a}$$

$$\sigma_h^2 \sim \mathbf{IG}(\underline{\nu}_h, \underline{S}_h) \tag{23a}$$

$$\sigma_g^2 \sim \mathbf{IG}(\underline{\nu}_g, \underline{S}_g) \tag{24a}$$

$$\sigma_{y^*}^2 \sim \mathbf{IG}(\underline{\nu}_{y^*}, \underline{S}_{y^*}) \tag{25a}$$

$$\sigma_{\pi^*}^2 \sim \mathbf{IG}(\underline{\nu}_{\pi^*}, \underline{S}_{\pi^*}) \tag{26a}$$

$$\sigma_\rho^2 \sim \mathbf{IG}(\underline{\nu}_{\rho\pi}, \underline{S}_\rho) \tag{27a}$$

$$\sigma_\lambda^2 \sim \mathbf{IG}(\underline{\nu}_\lambda, \underline{S}_\lambda) \tag{28a}$$

Prior on Initial States

The state vector contain trend inflation π_t^*, trend output y_t^*, time-varying inflation gap persistence ρ_t, time-varying slope of the Phillips curve λ_t, and the two log-volatility processes h_t(for the inflation equation) and g_t(for the trend block). As in Chan, Koop and Potter (2016), all state equations are driftless random walks, and we place relatively diffuse priors on the initial states.

For trend inflation, we center the initial state at the average of early sample inflation and allow for substantial uncertainty,

$$\pi_{t,1}^* \sim \mathrm{N}(\bar{y}_{1:4}, V_{\pi^*})$$

where $\bar{y}_{1:4}$ is the mean of the first four quarterly inflation observations. The prior variances V_{π^*} are set relatively large providing a fairly weakly informative but proper prior.

For trend output we use second difference formulation and treat the first two trend levels as noisy versions of the first observation of (scaled) real activity,

$$(y_1^*, y_2^*)' \sim \mathrm{N}((y_1, y_1)', diag(1/V_{y^*})$$

with $V_{y^*} = 1/y_1$ which yields a fairly diffuse prior on the initial level and slope of trend output.

The initial persistence of inflation gap is given a centered Gaussian prior,

$$\rho_1 \sim \mathrm{N}(0,1)$$

and the time-varying slope λ_t is treated symmetrically,

$$\lambda_1 \sim \mathrm{N}(0,1)$$

reflecting ex-ante uncertainty about the degree of inflation gap persistence and the strength of the real activity channel. In the sampler ρ_t is restricted to the stationary region, while λ_t is restricted to lie in $[0.05, 0.95]$at all dates. These constrains ensures a stationary inflation gap and a positive, procyclical Phillips-curve slope throughout, consistent with the use of an output-gap measure.

The initial log-volatility states h_1 and g_1 are assigned diffuse normal priors,

$$g_1 \sim \mathbf{N}(\mu_g, V_g), \quad h_1 \sim \mathbf{N}(\mu_h, V_h)$$

where $\mu_g = \mu_h = 1$ and $V_g = V_h = 10$. This implies moderate starting levels for conditional variances but allow the volatility processes to adapt flexibly to the data.

Priors for Output Gap

For the output gap we adopt the cyclical AR(2) specification and prior elicitation strategy proposed by Planas, Rosso and Fiorentini (2008). The cyclical component x_t of log(RGDP) is modelled as

$$x_t = \phi_1 x_{t-1} + \phi_1 x_{t-2} + \epsilon_t^x, \quad \epsilon_t^x \sim \mathbf{N}(\mathbf{0}, \sigma_x^2)$$

with the autoregressive polynomials having complex conjugate roots. Rather than placing priors directly on (ϕ_1, ϕ_2),we reparameterise the AR(2) process in terms of the modulus **a** and frequency (or period) τ of the complex roots. Under this parameterisation,

$$x_t = 2a\,cos(\tfrac{2\pi}{\tau})x_{t-1} - a^2 x_{t-2} + \epsilon_t^x \tag{29a}$$

so that the AR(2) coefficients are given by

$$\phi_1 = 2a\,cos(\tfrac{2\pi}{\tau})\ , \ \phi_2 = -a^2 \tag{30a}$$

The modulus $a \in (0,1)$governs the persistence of the cycle, while $\tau > 0$ controls its periods in quarters. This reparameterisation allows us to encode prior beliefs directly in terms of the economically meaningful characterstics of the business cycle rather than in terms of (ϕ_1, ϕ_2) where intuition is less transparent.

Following Planas, Rosso and Fiorentini (2008) we specify independent Beta priors for the persistence a and for a rescaled version of the period τ. For each country i,we assume (31a)

$$a_i \sim Beta(\alpha_{a,i}, \beta_{a,i,}),$$

with hyperparameters chosen so that $\mathbb{E}[a_i]$ lies in the range 0.7-0.8 and prior standard deviation is about 0.1, implying persistent but clearly mean reverting cycle. For the period τ_i,we restrict to the conventional business cycle band and define

$$\tau_i = \tau_{min} + B_i(\tau_{max} - \tau_{min})$$
$$B_i = Beta(\alpha_{\tau,i}, \beta_{\tau,i}),$$

where $\tau_{min} = 12$ and $\tau_{max} = 32$ quarters correspond to cycles between 3 and 8 years. The Beta hyperparameters $(\alpha_{\tau,i}, \beta_{\tau,i})$ are calibrated so that $\mathbb{E}[\tau_i]$ is close to the country specific business cycle frequency suggested by the literature and by preliminary univariate $AR(2)$ estimated for HP-filtered real GDP(around 4-5 years for Brazil, Chile and India). This contruction places most prior mass on stationary, cyclical dynamics with country specific but plausible durations, while ruling out very short lived, high frequency fluctuations and excessively long pseudo-trend components.

The Beta priors on (a_i, τ_i) induce a non-Gaussian prior on the $AR(2)$ coefficients $(\phi_{1,i}, \phi_{2,i})$ via nonlieanr mapping above. In practice, we follow Jarocinski and Lenza (2018) and approximate this induced prior by a bivariate Gaussian distribution. Specifically, for each country,

1. We draw a large Monte Carlo sample $\{(a_i^{(r)}, \tau_i^{(r)})\}_{r=1}^{R}$ from the Beta priors.
2. Transform these priors as shown in 30a into $(\phi_{1,i}^{(r)}, \phi_{2,i}^{(r)})$
3. Compute sample mean $m_{\phi,i} = \frac{1}{R} \sum_{r=1}^{R} \begin{pmatrix} \phi_{1,i}^{(r)} \\ \phi_{2,i}^{(r)} \end{pmatrix}$
4. Compute covariance $V_{\phi,i} = \frac{1}{R} \sum_{r=1}^{R} \left(\begin{pmatrix} \phi_{1,i}^{(r)} \\ \phi_{2,i}^{(r)} \end{pmatrix} - m_{\phi,i} \right) \left(\begin{pmatrix} \phi_{1,i}^{(r)} \\ \phi_{2,i}^{(r)} \end{pmatrix} - m_{\phi,i} \right)'$
5. Use $(\phi_{1,i}, \phi_{2,i})' \sim \mathcal{N}(m_{\phi,i}, V_{\phi,i})$ as the prior for output gap coefficients.

This approach preserves the Planas-Rossi-Fiorentini information in cycle length and persistence, while delivering a convenient Gaussian prior. It also ensures with high probability the output gap behaves as a smooth, stationary business cycle with countrry specific periodicity.

Posterior Simulators

Sample g

For sampling $g = (g_1, ..., g_T)'$ we will be using auxiliary mixture samplers of Kim, Shephard and Chib(1998). For sampling we will start with mixture indicators $s^g = (s_1^g, s_2^g, ..., s_T^g)$ by sampling it given the current g. After that we draw g given the mixture indicators.

For sampling g we will be using equations (5a),(13a) and (15a)

$$y_1^g = log(\pi_1^* - \mu_g)^2/V_g$$
$$y_t^g = log(\pi_t^* - \pi_{t-1}^*)^2 \text{ for } t = 2,3,....,T.$$

Mixture indicators $(s_1^g, s_2^g, ..., s_T^g)$ can be sampled sequentially as they are conditionally independent. For details please see (Kim, Shephard and Chib(1998)) and Chan et al. (2020). Given the mixture indicators s^g, we can sample g. First we transform equation(5a) in matrix form,

$$y^g = g + \epsilon^g$$
where $\epsilon^g \sim \mathbf{N}(d_{sg}, \Omega_{sg})$ and $y_g = (y_1^g, y_2^g, ..., y_T^g)$

Note that d_{sg} and Ω_{sg} are constant matrices which are determined by mixture indicators s^g from the table given in Kim, Shephard and Chib(1998).

The density function will be given as,

$$p(y^g|g, s^g) \propto exp(-\tfrac{1}{2}(y^g - d_{sg} - g)' \Omega_{sg}^{-1}(y^g - d_{sg} - g)$$

Now we write equation (13a), $g_t = g_{t-1} + \epsilon_t^g$ in the following matrix form,

$$Hg = u^g$$

$$H = \begin{bmatrix} 1 & 0 & 0 & . & . & . & 0 \\ -1 & 1 & 0 & . & . & . & 0 \\ 0 & -1 & 1 & 0 & . & . & 0 \\ . & . & . & . & . & . & . \\ . & . & . & . & . & . & . \\ . & . & . & . & . & . & 0 \\ 0 & 0 & 0 & . & . & -1 & 1 \end{bmatrix}$$

and u^g is normally distributed with mean $\widetilde{\mu_g}$ and variance S_g. Where we have $\widetilde{\mu_g} = (\mu_g, 0, ..., 0)$ and $S_g = diag(V_g, \sigma_g^2, .., \sigma_g^2)$;

Thus the prior density of g is given in the following manner,

$$p(g|\sigma_g^2) = -\tfrac{1}{2}(g - I_T\widetilde{\mu_g})' H' S_g^{-1} H(g - I_T\widetilde{\mu_g})$$

Finally solving the full conditional for g we get,

$$R_g = \Omega_{sg}^{-1} + H' S_g^{-1} H$$
$$\hat{g} = R_g^{-1}(\Omega_{sg}^{-1}(y^g - d_{sg}) + H' S_g^{-1} H 1_T \mu_g).$$

Sample h

We will proceed in the similar manner we sampled g using auxiliary mixture samplers of Kim, Shephard and Chib(1998). First we will sample the mixture indicators $s^h = (s_1^h,...,s_T^h)$ given h and other parameters. Then with the mixture indicators we sample h. Then s^h is drawn in the same manner as for s^g.

Here we will be using (2a),(11a) and (16a). First we write (2a) in matrix form,

$$y^h = h + \epsilon^h$$

where $y_t^h = log((\pi_t - \pi_t^*) - \rho_t(\pi_{t-1} - \pi_{t-1}^*) - \lambda_t x_t)$; $\epsilon^h \sim N(d_{s^h}, \Omega_{s^h})$ and $y^h = (y_1^h,...,y_T^h)$.

Then we transform (11a) as,

$$Hh = u^h$$

where $u^h \sim N(\widetilde{\mu_h}, S_h)$. We have $\widetilde{\mu_h} = (\mu_h, 0, 0..., 0)'$; $S_h = diag(V_h, \sigma_h^2, .., \sigma_h^2)$. We derive the rest using the same routine as for g and we get,

$$R_h = \Omega_{sh}^{-1} + H' S_h^{-1} H$$
$$\hat{h} = R_h^{-1}(\Omega_{sh}^{-1}(y^h - d_{sh}) + H' S_h^{-1} H 1_T \mu_h).$$

Sample π^*

For sampling π^* we will be using equations (2a) and (5a) and find the log density and solve ignoring terms not including π^*.

We will first rewrite (2a) as

$$M_\rho \pi = \delta_\pi + M_\rho \pi^* + \epsilon^\pi$$
$$M_\rho = \begin{bmatrix} 1 & 0 & 0 & . & . & . & 0 \\ -\rho_2^\pi & 1 & & & & & 0 \\ 0 & -\rho_3^\pi & 1 & & & & 0 \\ . & & . & 1 & & & . \\ . & & & . & & & . \\ . & & & & . & & . \\ 0 & 0 & . & . & . & -\rho_T^\pi & 1 \end{bmatrix} \quad \delta_\pi = \begin{bmatrix} \rho_1^\pi(\pi_0 - \pi_0^*) + \lambda_1(y_1 - y_1^*) \\ \lambda_2(y_2 - y_2^*) \\ \lambda_3(y_3 - y_3^*) \\ . \\ . \\ . \\ \lambda_T(y_T - y_T^*) \end{bmatrix} \tag{2b}$$

$\epsilon^\pi \sim N(0, \Omega_\pi)$ where $\Omega_\pi = diag(e^{h_1}, e^{h_2}, ..., e^{h_T})$. Note here M_ρ is invertible as $|M_\rho| = 1$ for any ρ

So the log density that we get is (2c)

$$log\, p(\pi|y,y^*,\rho^\pi,\lambda,h,\theta) \propto -\tfrac{1}{2} i_T' h - \tfrac{1}{2}(\pi - M_\rho^{-1}\delta_\pi - \pi^*)' M_\rho' \Omega_\pi^{-1} M_\rho (\pi - M_\rho^{-1}\delta_\pi - \pi^*)$$

Now we rewrite (5a) as

$$H\pi^* = \epsilon^{\pi^*} \tag{5b}$$

where $\epsilon^{\pi^*} = (m_{\pi^*}, S_{\pi^*)}$

$S_{\pi^*} = diag(e^{g_1} V_{\pi^*}, e^{g_2}, .., e^{g_T})$
$m_{\pi^*} = (\mu_{\pi^*}, 0, 0, .., 0);$

$$H = \begin{bmatrix} 1 & 0 & 0 & . & . & . & 0 \\ -1 & 1 & 0 & . & . & . & 0 \\ 0 & -1 & 1 & 0 & . & . & 0 \\ . & . & . & . & . & . & . \\ . & . & . & . & . & . & . \\ . & . & . & . & . & . & 0 \\ 0 & 0 & 0 & . & . & -1 & 1 \end{bmatrix}$$

Finally combing equation (2c) and (5b). We only use the variables with π^* and do not consider others. Finally we get

$R_{\pi*} = (H' S_{\pi^*}^{-1} H + M_\rho' \Omega_\pi^{-1} M_\rho)^{-1}$
$= \hat{\pi}^* = R_{\pi^*}(H' S_{\pi^*}^{-1} m_{\pi^*} + M_\rho' \Omega_\pi^{-1} M_\rho (\pi - M_\rho^{-1}\delta_\pi))$

Sample from $p(y^*|y,y^*,\rho^\pi,\lambda,h,\theta)$

For sampling y^* we will be using equation (2a),(3a),(4a) and (6a) and find the log density and solve ignoring terms not including y^*.

First we rewrite (2a) as,

$m = \Lambda y^* + \epsilon^\pi$

where $m_t = (\pi_t - \pi_t^*) - \rho_t(\pi_{t-1} - \pi_{t-1}^*) - \lambda_t y_t$;

$\epsilon^\pi \sim N(0, \Omega_\pi)$ and $m = (m_1, m_2, ..., m_T)$, $\Lambda = diag(-\lambda_1, -\lambda_2, ..., -\lambda_T)$

$$log\, p(\pi|y_t,y_t^*,\rho,\lambda,h,\theta) \propto -\tfrac{1}{2}(m - \Lambda y^*)' \Omega_\pi^{-1} (m - \Lambda y^*)' \tag{2b}$$

Secondly we rewrite (3a) and (4a) as

$$y = y^* + x$$

$$Q_y y = \beta_y + Q_y y^* + \epsilon^y$$

where $\epsilon^y \sim N(0, \Omega_y)$ $\beta_y = [\phi_1(y_0 - y_0^*) + \phi_2(y_{-1} - y_{-1}^*); \phi_2(y_0 - y_0^*); 0; 0; ....; 0]$

$$\Omega_y = I_T \otimes \sigma_y^2$$

$$Q_y = \begin{bmatrix} 1 & 0 & 0 & . & . & . & 0 \\ -\phi_1 & 1 & 0 & . & . & . & 0 \\ -\phi_2 & -\phi_1 & 1 & 0 & . & . & 0 \\ 0 & -\phi_2 & -\phi_1 & 1 & . & . & 0 \\ . & . & . & . & . & . & . \\ . & . & . & . & . & . & . \\ 0 & . & . & . & -\phi_2 & -\phi_1 & 1 \end{bmatrix}$$

$$log\, p(y|y^*, \theta) \propto \tfrac{1}{2}(y - Q_y^{-1}\beta_y - y^*)' Q_y' \Omega_y^{-1} Q_y (y - Q_y^{-1}\beta_y - y^*) \tag{2c}$$

Finally we rewrite (6a) as,

$$H_2 y^* = \hat{\alpha}_{y^*} + \epsilon^{y^*} \text{ where } \hat{\alpha}_{y^*} = (y_0^* + \Delta y_0^*, -y_0^*, 0, ..., 0);$$

$$\text{and } H_2 = \begin{bmatrix} 1 & 0 & 0 & . & . & . & 0 \\ -2 & 1 & 0 & . & . & . & 0 \\ 1 & -2 & 1 & 0 & . & . & 0 \\ . & . & . & . & . & . & . \\ . & . & . & . & . & . & . \\ . & . & . & . & . & . & 0 \\ 0 & 0 & 0 & . & 1 & -2 & 1 \end{bmatrix}$$

Let $\alpha_{y^*} = H_2^{-1}\hat{\alpha}_{y^*} = (y_0^* + \Delta y_0^*; y_0^* + 2\Delta y_0^*; ....; y_0^* + T\Delta y_0^*)$

where $\epsilon^{y^*} \sim N(0, \Omega_{y^*})$ where $\Omega_{y^*} = diag(V_{y^*}, \sigma_{y^*}^2, ..., \sigma_{y^*}^2)$

$$log\, p(y^*|\sigma_{y^*}^2) \propto -\tfrac{1}{2}(y^* - \alpha_{y^*})' H_2' \Omega_{y^*}^{-1} H_2 (y^* - \alpha_{y^*}) \tag{2d}$$

We will combine equations (2b), (2c) and (2d). We will only use the variables with y^* and do not consider others. Hence we get

$$R_{y^*} = (Q_y' \Omega_y^{-1} Q_y + H_2' \Omega_{y^*}^{-1} H_2 + \Lambda' \Omega_\pi^{-1} \Lambda)^{-1}$$
$$\hat{y^*} = R_{y^*}(\Lambda' \Omega_\pi^{-1} m + Q_y' \Omega_y^{-1} Q_y (y - Q_y^{-1}\beta_y) + H_2' \Omega_{y^*}^{-1} \alpha_{y^*})$$

Sample from $p(\rho|y,\pi^\tau,x^\tau,\lambda,h,\theta)$

For sampling $p(\rho|y,\pi^\tau,x^\tau,\lambda,h,\theta)$ we will be using equation (2a) and (7a) and find the log density and solve ignoring terms not including ρ^π.

Equation (2a) can be rewritten as,

$$\tilde{\pi} + \Lambda\tilde{y} = Z_\pi\rho^\pi + \epsilon^\pi$$

where $\epsilon_\pi \sim N(0,\Omega_\pi)$; $\tilde{\pi}_t = (\pi_t - \pi_t^*), \tilde{y}_t = (y_t - y_t^*)$

$\tilde{\pi} = (\tilde{\pi}_1,\tilde{\pi}_2,...,\tilde{\pi}_T)$; $(\tilde{y} = \tilde{y}_1,\tilde{y}_2,....,\tilde{y}_T)$; $Z_\pi = diag(\tilde{\pi}_0,\tilde{\pi}_1,....,\tilde{\pi}_{T-1})$; $\Lambda = diag(-\lambda_1,-\lambda_2,...,-\lambda_T)$
$\Omega_\pi = diag(V_\rho,\sigma_\rho^2,..,\sigma_\rho^2)$;

Equation (7a) can be written as,

$$H\rho^\pi = \alpha_\rho + \epsilon^\rho$$

where $\epsilon^\rho \sim N(0,\Omega_\rho)$, $\alpha_\rho = (\rho_0,0,...,0)$; $\Omega_\rho = diag(V_\rho,\sigma_\rho^2,....,\sigma_\rho^2)$

Where $0 < \rho_t < 1$ for $t = 1:T$,

$$f_\rho(\rho,\sigma_\rho^2) = -\sum_{t=2}^{T} log(\Phi(\tfrac{1-\rho_{t-1}}{\sigma_\rho}) - \Phi(\tfrac{-\rho_{t-1}}{\sigma_\rho}))$$

Using the same procedures as above we get,

$$M_\rho = (H'\Omega_\rho^{-1}H + Z_\pi'\Omega_\pi^{-1}Z_\pi)^{-1}$$
$$\hat{\rho} = M_\rho Z_\pi'\Omega_\pi^{-1}(\tilde{\pi} + \Lambda\tilde{y})$$

Sample $p(\lambda|y,\pi^\tau,x^\tau,\rho,h,\theta)$

For sampling $p(\lambda|y,\pi^\tau,x^\tau,\rho,h,\theta)$ we will be using equation (2a) and (9a) and find the log density and solve ignoring terms not including λ.

We can rewrite (2a) as ,

$$j = \lambda\widetilde{Y} + \epsilon^\pi$$

where $j = (\tilde{\pi}_1 - \rho_1\tilde{\pi}_0;.....;\tilde{\pi}_T - \rho\tilde{\pi}_{T-1})$, $\tilde{Y} = diag(\tilde{y}_0,\tilde{y}_1,...,\tilde{y}_{T-1})$ and $\lambda = (\lambda_1,...,\lambda_T)$.

So the log density that we get is,

$$(\pi_t|\pi^*,y_t,y_t^*,\lambda,h) \propto -\tfrac{1}{2}(j - \lambda\widetilde{Y})'\Omega_\pi^{-1}(j - \lambda\widetilde{Y})$$

Next we write (9a) in the first difference form as shown in earlier cases,

$$H\lambda = \alpha_\lambda^* + \epsilon^\lambda$$

where $\alpha_\lambda^* = (\lambda_0,0,...,0)$ and $\Omega_\lambda = diag(V_\lambda,\sigma_\lambda^2,\sigma_\lambda^2....,\sigma_\lambda^2)$.

So $\lambda|\sigma^2 \sim N(\beta_\lambda, (H^{'}\Omega_\lambda^{-1}H)^{-1})$

Where $0 < \lambda_t < 1$ for $t = 1:T$,

$f_\lambda(\lambda, \sigma_\lambda^2) = -\sum_{t=2}^{T} log(\Phi(\frac{1-\lambda_{t-1}}{\sigma_\lambda}) - \Phi(\frac{-\lambda_{t-1}}{\sigma_\lambda}))$

After solving as in earlier cases,

we get $M_\lambda = (H^{'}\Omega_\lambda^{-1}H + \tilde{Y}^{'}\Omega_\pi^{-1}\tilde{Y})^{-1}$

and $\hat{\lambda} = M_\lambda \tilde{Y}^{'}\Omega_\pi^{-1}j$

Sample ϕ

From (4a), note $\phi = [\phi_1, \phi_2]$

$$\tilde{Y} = \begin{bmatrix} \tilde{Y}_0 & \tilde{Y}_{-1} \\ \tilde{Y}_1 & \tilde{Y}_0 \\ & \\ & \\ \tilde{Y}_{T-1} & \tilde{Y}_{T-1} \end{bmatrix}$$

We will be assuming that the following stationary constraints will be holding,

$\phi_1 + \phi_2 < 1$

$\phi_1 - \phi_2 < 1$

$|\phi_2| < 1$

Applying similar routines as in earlier cases we get,

$M_\phi = (V_\phi^{-1} + \tilde{Y}^{'}\tilde{Y}/\sigma_y^2)^{-1}$

$\hat{\phi} = M_\phi \tilde{Y}^{'}/\sigma_y^2$

Sample Γ

Where $\Gamma = (y_0^*, y_{-1}^*)$

We will write y^* in (6a) in matrix form as,

$$y^* = X_{y^*}\Gamma + H_2^{-1}\epsilon^{y^*}$$

where

$$X_\Gamma = \begin{bmatrix} 2 & -1 \\ 3 & -2 \\ . & . \\ . & . \\ T+1 & -T \end{bmatrix} \quad \text{and hence } X_\Gamma\Gamma = \begin{bmatrix} y_0^* + \Delta y_0^* \\ y_0^* + 2\Delta y_0^* \\ . \\ . \\ y_0^* + T\Delta y_0^* \end{bmatrix}$$

Similar to earlier routines we get,

$$R_{y^*} = V_\Gamma^{-1} + \tfrac{1}{\sigma_{y^*}^2} X_\Gamma' H_2' H_2 X_\Gamma.$$
$$\hat{\Gamma} = R_{y^*}^{-1}(V_\Gamma^{-1}\Gamma_0 + \tfrac{1}{\sigma_{y^*}^2} X_\Gamma' H_2' y^*)$$